Republic of Iraq
Ministry of Higher Education
And Scientific Research
University of Babylon / College of Science
Department of Physics

Preparation and characterization of (PMMA- MWCNT) thin films and their application as gas sensor

A-Thesis

Submitted to the Council of College of Science University of Babylon as a Partial Fulfillment of the Requirements for the Degree of Master in Science / Physics

By

Mohammed Hatif Salih Mahdi

B.Sc. in Physics/ (2007)

Supervised by

Prof. Dr.
Mohammed Hadi Shinen

Asst. prof. Dr.
Maan Abd-Alameer Salih

2022 A.D. **1444 A.H.**

بِسْمِ اللَّهِ الرَّحْمَنِ الرَّحِيمِ

{ وَيَسْأَلُونَكَ عَنِ الرُّوحِ قُلِ الرُّوحُ مِنْ أَمْرِ رَبِّي وَمَا أُوتِيتُم مِّن الْعِلْمِ إِلاَّ قَلِيلاً }

صَدَقَ اللهُ العَلِيُّ العَظيم

(سورة الاسراء:الآية ٨٥)

Dedication

I dedicate this effort

TO

Dears

To my Father,

My Mother,

My Wife,

My brothers, my sisters,

My son and daughter

With all my gratitude

MOHAMMED

Supervisors Certification

We certify that this thesis entitled **(Preparation and characterization of (PMMA - MWCNT) thin films and their application as gas sensor)** was prepared by **(Mohammed Hatif Salih Mahdi)** under our supervision at the Physics Department in the College of Sciences, University of Babylon, as a partial fulfillment of the requirements for the degree of M.Sc. in Physics.

Signature :

Supervisor : Dr. Mohammed Hadi Shinen

Title : Professor

Address : University of Babylon / College of Science / Department of Physics

Date : / / 2022

Signature :

Supervisor : Dr. Maan Abd-Al ameer Salih

Title : Assistant Professor

Address : University of Babylon / College of Science / Department of Physics

Date : / / 2022

Certification of the Head of the Department

In view of the available recommendations, I forward this thesis for debate by the examination committee.

Signature:

Name : **Dr. Samira Adnan Mahdi**

Title : Asst. Prof

Address: Head of Department of Physics, College of Sciences, University of Babylon.

Date : / / 2022

Examining Committee Certification

We certify that we have read this thesis entitled **(Preparation and characterization of (PMMA - MWCNT) thin films and their application as gas sensor)** and in our opinion as an examining committee examined the M.Sc. student **" Mohammed Hatif Salih Mahdi "** in the contents, it is adequate with **(very good)** as a thesis meets the standard for the degree of Master in physics.

Signature**:**
Name**: Dr. Fouad Shakir Hashim**
Title: Professor
Address: University of Babylon - College of Science - Department of Physics.
Date: / /2022
(Chairman of the Committee)

Signature**:**
Name**: Dr. Ali Qassim Abdullah**
Title: Professor
Address: University of Basra - College of Science - Department of Physics.
Date: / /2022
(Member)

Signature**:**
Name**: Dr. Nassar Abdulameer Al-Isawi**
Title: Lecturer
Address: University of Babylon - College of Science - Department of Physics
Date: / / 2022
(Member)

Signature**:**
Name**: Dr. Mohammed Hadi Shinen**
Title: Professor
Address: University of Babylon - College of Science - Department of Physics.
Date: / /2022
(Member and Supervisor)

Signature**:**
Name**: Dr. Maan Abd-Alameer Salih**
Title: Asst. prof. Dr.
Address: University of Babylon - College of Science - Department of Physics.
Date: / /2022
(Member and Supervisor)

Approved by the College of Science Committee on Graduate Studies.

Signature:
Name**: Dr. Mohammed Mansour Kadhum AlKafaji**
Title: Professor
Address: Dean of College of Science – University of Babylon
Date: / /2022

ACKNOWLEDGMENTS

First of all, my deepest gratitude goes to ALLAH (the Almighty), the compassionate, and the merciful for everything.

I would like to enlarge my thanks and gratitude to my supervisor, Prof. Dr. Mohammed Hadi Shinen and Assist. Prof. Dr. Maan Abd-Alameer Salih for having optional this topic for me and for their distinguished labors, sound advice and orders that have helped in smoothing out every complexity encountered through my vocation.

Many thanks to the Deanery of the College of Science in Babylon University and the Department of Physics for giving me the chance to complete my study.

I am very grateful to Dr. Ali Jabbar Khalaf for his help throughout the research work.

Finally, I would like to thank all the members of my family for their help and support and everyone who helped me during the preparation of this thesis. Also, I would also like to thank all those who have supported me with his sincere invitations or sincere wishes. I thank them all and I hope that God will make that in the balance of their merits.

MOHAMMED

Summary

In this study, PMMA solution with multi-wall carbon nanotubes were prepared with different concentration ratio of about (1, 3 and 5) wt % The composites, then have been studied by (FTIR) to determine the active groups of the chemical bonds. The results of the analysis showed that the polymer is Poly (methyl methacrylate), also showed that the doping did not affect the characteristics of Poly (methyl methacrylate).

The X- ray diffraction (XRD) results showed that the prepared films are amorphous for the pure polymer and the doping didn't effect synthetic properties of Poly (methyl methacrylate).

The surface morphology of thin films was examined using the atomic force microscope technique (AFM). The results showed that the prepared films were homogeneous. The roughness average, the Root Mean Square (RMS) decreases and the average grain size increased with the increasing of (MWCNTs) concentration.

The optical properties of the prepared films were investigated by obtaining the transmittance spectra in the UV- VIS regions as a function of wavelength from (200-1000) nm. Optical properties including absorbance and transmittance spectra as a function of wavelength have been measured as well as the absorption coefficient and other optical constants. The values of absorbance, absorption coefficient and refractive index values of pure and doped polymer are increasing with the increasing of the concentration ratios of MWCNTs. The results showed decreases in the values of transmittance with all concentration ratios of MWCNTs. The values of reflectance are increased with the increasing of concentration ratio; also, results showed decreasing of energy gap for allowed direct transition with increasing of doping ratio. The energy gap values were obtained and were equal to 3.52 -3.88 eV for pure polymer with different rates of carbon nanotubes.

For pure and doped thin film, it noted that with increasing doping concentration the sensitivity for two types of gases (NO_2, NH_3) is increased because with increasing doping concentration the average grain size increases and the roughness of surface decreases leading to increases in the sensitivity of film.

Table of Contents

List of Symbols

Symbols	*Physical meaning*	*Unite*
A	Absorbance	
λ	Wavelength	(nm)
α	Linear Absorption Coefficient	(cm^{-1})
ΔE	The Excitation Energy for Radiation	(cm^{-1})
A_{ki}	The Probability of Transition from the Upper States to the Lower States	(s^{-1})
T	Transmittance	
R	Reflectance	-
D	Average grain size	nm
d_{hkl}	Miller indices	-
n	Refractive Index	
E_{exc}	Excitation Energy of Upper Level	(cm^{-1})
k_o	Extinction Coefficient	(cm^{-1})
FWHM	Full Width at Half Maximum	(nm)
h	Plank's Constant = (6.62×10^{-34})	($J\ s^{-1}$)
E	Dielectric Constant	
$h\upsilon$	Photon energy	eV
I	Intensity of Laser	(W/cm^2)
I	Current	A
K_B	Boltzmann's constant = (1.38×10^{-23})	(J/K)
m_e	Electron Mass = (9.108×10^{-31})	(kg)
m_p	Proton Mass = (1.67×10^{-27})	(kg)
$E_g^{opt.}$)	optical energy gaps	eV
Q.E (λ)	Quantum Efficiency at Wavelength λ	(%)
α_{IB}	Inverse- Bremsstrahlung Absorption Coefficient	(cm^{-1})
ε_o	Permittivity of Free Space = (8.854×10^{-14})	(F/m)
P	Charge Density	(cm^{-3})
Ra	electric resistances in gas	Ω
Rg	electric resistances in air	Ω
2θ	Bragg diffraction angle	Degree

Abbreviations

Symbols	*Physical meaning*
MWCNT	multi-walled carbon nanotube
PMMA	Poly methyl methacrylate
CNDs	Carbon Nano- dots
SWCNTs	Single walled carbon nanotubes
CNTs	Carbon Nanotubes
A FM	Atomic Force Microscopy
PHB	poly(3-hydroxybutyrate)
FTIR	Fourier Transform Infrared
RMS	Root Mean Square
FWHM	Full Width at Half Maximum
V.B	Valence Band
UV	Ultra Violet
VIS	Visible
XRD	X-Ray Diffraction
CB	Conduction Band
V.I.S	Visible Spectrum

List of Figures

List of Table

Chapter One

Introduction

And

Literature Review

1.1 General Introduction

The field of materials science and technology is considered the most enormous and challenging areas of science in both branch of old and new advance science. Materials science is a field cover the oldest history and even named it such (Bronze Age, Iron Age, etc.) and represent the steps approach to break through developments in the whole life [1].

Recent material emerged due to requirement to enhance the effectiveness of structure and its operation, and others initiated a different area to design enhanced designs and technologies. Such processes in developing required material, structure design, and technologies are related to composite material. It is seen as a great manifestation [2].

Solid materials could be divided into many sets depending on their chemical bonds, which found between the atoms and molecules in addition them depending on these atomic structures so the researchers classified materials into three main group's metal, ceramic and polymers. Composite material considered an intermediate classification of solid-state material, which consists of two or more combined materials [3].

Using Nanotechnology has been initiated in about 50 years ago due to the easiness of dealing with the materials using nanometer scales. Nanotechnology allows to control the features of the matters through manipulations and observations of atoms. It got a great interest by scholars in the field in the recent years due to its capability to be used in different fields such as medicine, industry, pollution treatments etc. [4].

Its major norm is to reduce the volume of the atom to have much efficiency and less consuming, beside the capability to show high quality of electronic, optical and magnetic features. Carbon is available in great quantities on earth having different forms like carbon nanotubes (CNT), fluorine, and graphene [5].

CNT has received a great interest because of its great features like its light weight, high chemical and thermal stability beside having a vital role in the preparation of nanocomposites [6].The electrical, mechanical properties and optical of CNT/polymer composites are an area of extensive research. The structural element in nanocomposites is the presence of nanotubes which improves the properties of materials and thus in optoelectronics found a variety of applications, strengthening materials, etc [7]. The electrical properties of the composites have been explained by several authors in a dielectric polymer matrix, carbon nanotubes are dispersed such as epoxy, phoenix polyimide, resin, etc. based on filtration theory [8,9].

1.2 Polymer:

The polymer is a Latin word consisting of (poly), which means plural and (mer), meaning part, meaning multi-part. The polymer molecule is a large molecule with a high molecular weight ranging from 104000-106000 g /mol [10]. It is made up of small chemical molecules that are bound together by chemical bonds. These molecules may bind for one other linearly [11]. The polymeric molecule is sometimes called a branched polymer each of which in the chain may has a comb-shaped or ladder shape or cruciform. They might have variable sizes and sometimes intertwined (the cross- linked polymer). The Different types of polymer chains are shown in Figure (1.1) [12].

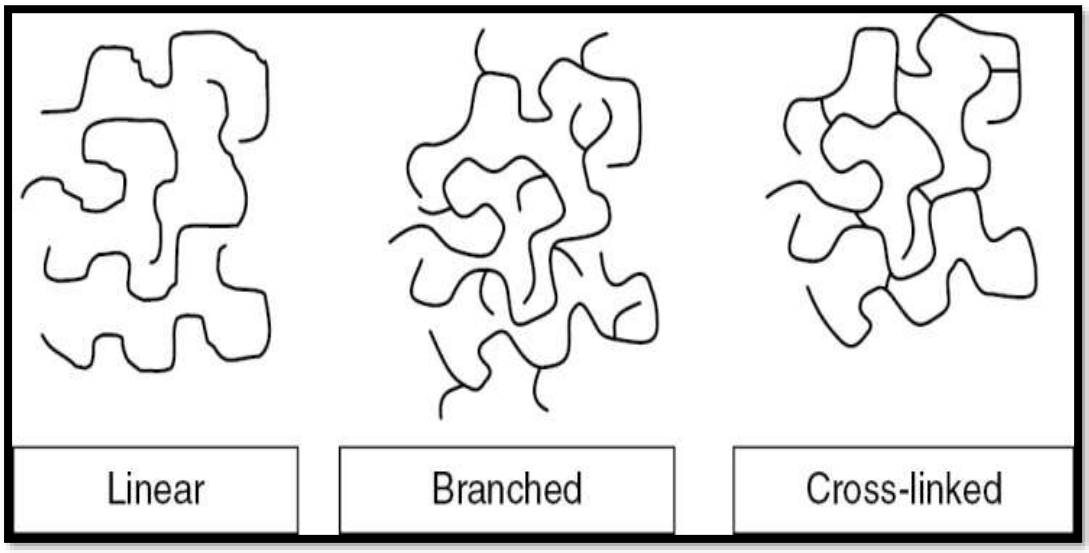

Fig. (1.1) The sorts of polymer chains [12].

The degree of crosslinking has a significant effect on physical properties of polymer. As the degree of crosslinking decreases, the properties of the rubber increase, the melting point increases, and the polymer become insoluble, non-conductive, thermal and electrical [13]. The simple molecule that consists of a polymer molecule is called a monomer (a simple chemical compound with a small molecular weight). Characterized by a special structure that can react with another molecule of the same type or another compound molecule under the appropriate conditions to form a chain polymer, the monomer is a procured formula called the repeating unit or the structural unit of the polymer encapsulated in brackets[14].

1.3 Polymerization and Methods of Preparing Polymers:

Any process consisting of very small molecules that combine with each other relatively, polymerization, the monomers are called a polymer that is the production of very large network or chain molecule. Monomer molecules maybe the same, or different where there are two, three, or more different compounds. Where several thousand in one polymer molecule monomer units are combined.

Sometimes as many as one hundred monomer molecules are built to make a product with distinct and specific ability to form fibers, or high tensile strength, Polymers are distinguished from materials made of smaller, simpler particles by their physical properties they represent weak forces affect a large number of intermolecular macromolecules crystallization is formation of stable chemical covalent bonds between monomers, by which polymerization is distinguished from any other form of process [15].

There are two types of polymerization; condensation polymerization is one type of polymerization in which each step takes place to form a molecule of a simple structure, usually water, beside polymerization, the reaction of monomers occurs to make a polymer without it, usually accompanied with the formation of the product.. Addition polymerization is usually performed In the presence of certain catalysts, characteristically affecting the properties of the polymer which in some cases controls the structural details [16].

1.3.1 Condensation Polymerization:

Condensation polymerization is a type of polymerization that falls under gradual Polymerization occurs in which monomers and/or oligomers interact with each other and larger structural units are formed. and release smaller molecules as a by-product such as methanol or water[17].

Esterification of carboxylic acids with alcohols is one example of a condensation reaction. If there is a difference in the two slits, the condensation product is a linear polymer, and if at least one of the slits is triangular or quadrilateral, then crosslinking of the resulting polymer will occur (i.e. a three-dimensional network).The growth chain is terminated

by adding monomers with only one reactive group, so the average molecular weight will decrease.

Crosslinking density and average molecular weight will have defining factors to then depend on such as the function and property from each monomer present and participating in the condensation polymerization and the percentage of its concentration in the mixture [18]. Repeat units are produced by preparing condensing polymers typically through the reaction of two homologous bifunctional monomers, however, when another symmetric monomer is added to the polycondensing system in an attempt to prepare a repeating unit chain polymer, the situation becomes very complex.

1.3.2 Addition Polymerization:

When the monomers are reacted, a polymer is formed without by-products being formed, in addition to the polymerization. Addition polymerization is usually performed in the presence of certain catalysts; in some cases they control structural details that importantly influence the properties of the polymer. It is named as " chain growth polymerization" or "addition polymerization"[19]. It is applied to vinyl monomers (ie those having a carbon-carbon double).Ligands and some sorts of cyclic monomers (i.e., containing the double bond in the form of a ring). The other process, called gradual growth polymerization, involves. Additional polymerization reactions are described, it is also exothermic, that is, it generates and produces heat. Small reactions such as heat generation are seldom a problem but at other scales such as the large industrial scale, it can be a source of danger, because heat is an important factor in increasing the reaction rate and faster reactions [20].

1.4 Classification of polymers:

Polymers can be classified into natural or synthetic based on their origin and others according to functions, source, polymerization mechanism, polymer structure, preparation techniques, and thermal behaviour. This information describes a system for classifying natural polymers according to their sources. Some of the most widely used natural polymers in industries are discussed. Such as proteins, polyisoprene, sugars, nucleotides, and polyester [21].

1.5 Physical Properties of Polymer:

Polymers are substances found in nature. Its basic molecular structure is very similar to that of most plant and animal forms. Silk, shellac, bitumen, rubber and cellulose are natural polymers. There are many beneficial properties of polymers that are unique to polymers. It has several properties that include the physical properties of polymers such as molar size, molecular weight, density, Polymerization value, crystallization of the material, and also its molecular structure that distinguishes it from being long chain[22].

1.6 Methods of preparation polymer thin film:

Many techniques produce fine polymeric films and there are two methods for preparing ultra-thin organic and polymeric films: the first includes wet processes such as diffusion, Langmuir Blodgett, Dipping molding or solvent methods (spin casting). Also, dry processing, such as plasma polymerization, chemical vapour deposition, spraying, vapour deposition or vapour deposition polymerization methods, among these methods, is the application of optical and electronic package resistors to silicon wafers, one of the most common methods of polymeric film solvents[23].

1.7 Poly methyl methacrylate (PMMA) Polymer:

The trade names of poly methyl methacrylate are PMMA, Plexiglas, Lucite; the family class is vinylidene polymers (acrylics). The chemical formula of PMMA structure is [23]:

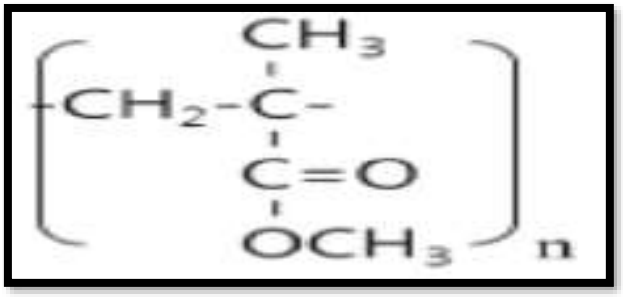

Fig. (1.2) The Chemical structure of PMMA[23].

PMMA is a thermoplastic material (see Fig. (1.2)) that got a great interest recently because of its low cost, good strength, and hardness, high rigidity, transparency, and many other qualities that makes it very valuable for many products[24]. PMMA has natural transparence that is equal to (92 wt.%), good optical and mechanical features with no color. It is used in a variety of industries and domestic fields because of its magnificent physical and optical features like replacing glass in different fields and nowadays it is employed in glazing applications. It could be classified as good in hosting organic nano particles because of the high surface to bulk ratio that could be highly affective for the features of PMMA matrix. Polymeric composite of PMMA is known in its vital role in technology [25]. PMMA is used in several applications, it can used instead of glass as well as can be used in component deep UV and as a resistance for electron beam or ion-beam resists in microelectronics chips manufacturing, Sensor applications [26]. Poly methyl methacrylate is composed by free radical polymerization of methyl methacrylate in mass or suspension polymerization The PMMA is considered an amorphous material because of the methyl ester pendant groups, which block the

crystallization by preventing molecules to form crystalline bonds with each other [26].

1.8 Carbon Nanotubes (CNTs):

A type of carbon allotrope made by graphite appearing as cylindrical tubes with a diameter of up to nanometers and a length of up to millimeters. It is known that sp^2 hybridized carbon forms planar structures with a complicated interlocking, which is dependent on the hexagonal ring arrangements [27]. CNT has great features like chemical stability [28]. Thus, it got great interest in different fields due to its vital importance for different uses, products, and applications [29]. Recently, carbon nanotube has started to be employed as greatly efficient templates for hybrid with other nanoparticles (NPs) because of its capability in maintaining structures as well as the morphologies because they are greatly hard. Due to its open-ended structure in both sides so that the inside surface could be reached easily which gives good opportunities for integrating the Nano types in the nanotubes [30].

Besides that, CNTs have the ability of entering the cells in an easy way because of their tubular shapes with high flexibility. Producing them is done in several ways such as chemical vapor deposition (CVD), hydrothermal processes, plasma rotating etc. Carbon nanotubes are classified according to the number of layers: single-walled nanotubes (SWNTs) and multi-walled nanotubes (MWNTs). This indicates that they have very good qualities like very light weight and high thermal conductivity, which allow them to be use in a variety of applications in different fields [31].

1. 9 Single-Walled Carbon Nanotubes (SWCNTs):

Single walled carbon nanotubes (SWCNTs) are composed of one layer of graphite wrapped on each other in a cylindrical shaped that is open from the sides having a tree –shape structure[32]. Its diameter is (0.4-2) nm depending on the temperature of growth. The higher the temperature the bigger the diameter of the nanotubes. Carbon nanotubes are bonded in a weak way to each other via van der Waals interaction. Single walled carbon nanotubes (SWCNTs) have some arrangements: zigzag, armchair, helical, chiral as illustrated in Figure (1.3) [33]. Due to the strong and high surface area, it is employed in several products and applications in both drugs and biosynthesis fields. SWCNTs are metallic with high electrical conductivity or semiconductors with exceptional tensile strength because of the nanostructure and strength of the bonds among carbon atoms [33].

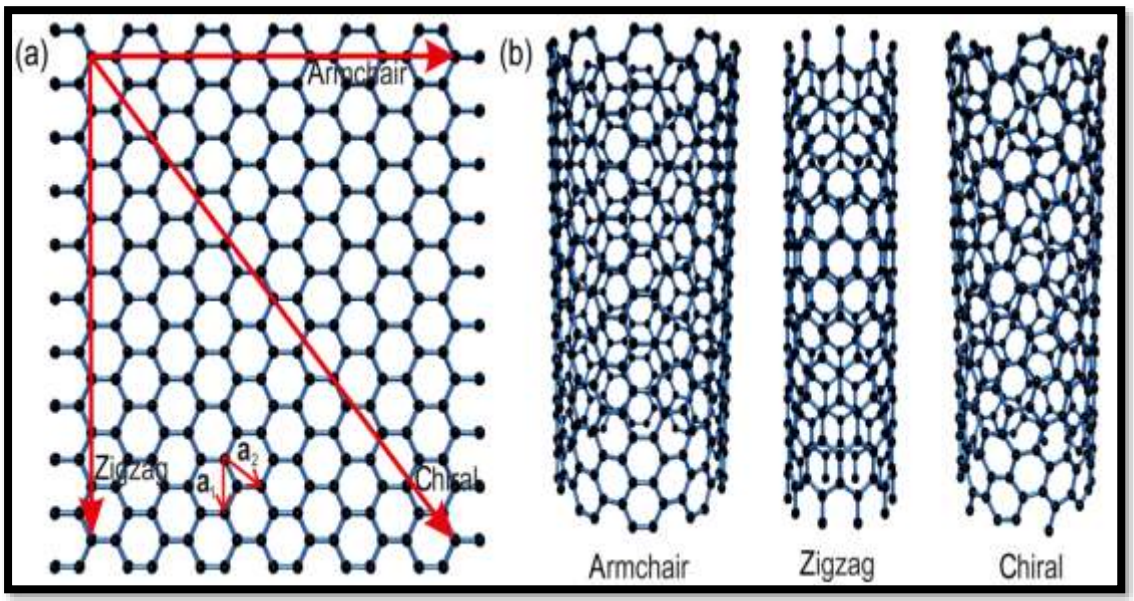

Fig. (1.3): The Schematic structure of (a) graphene sheet, (b) SWCNT [33].

1.10 Multi -Walled Carbon Nanotubes (MWCNTs):

MWCNTs are composed of some layers of bounded graphene on each other with a cylindrical shape (concentric tubes) (Figure 1-4). The inside diameter of the nanotubes ranges between (1-3) nm and the outer one ranging between (2-100) nm. The length is only some micrometers [34]. Their structure is illustrated in two ways: firstly, the Russian doll model that is the wrapped graphene sheets in a concentric structure. Secondly, the parchment which is wrapped graphene sheet around itself several times like a rolled newspaper [34]. Since it has the largest number of layers, carbon nanotubes could compose a protection for the inner tubes from chemical reactions with external materials with high tensile strength that is distinguishing them from SWCNTs. The interlayer distance between the carbon nanotube layers is up to 0.34nm is closer to the distance between the graphene layers in polyaromatic solids. The high ability to decoration with nanoparticles (NPs) and maintaining the structures got them within the scope of the researchers' interests [35].

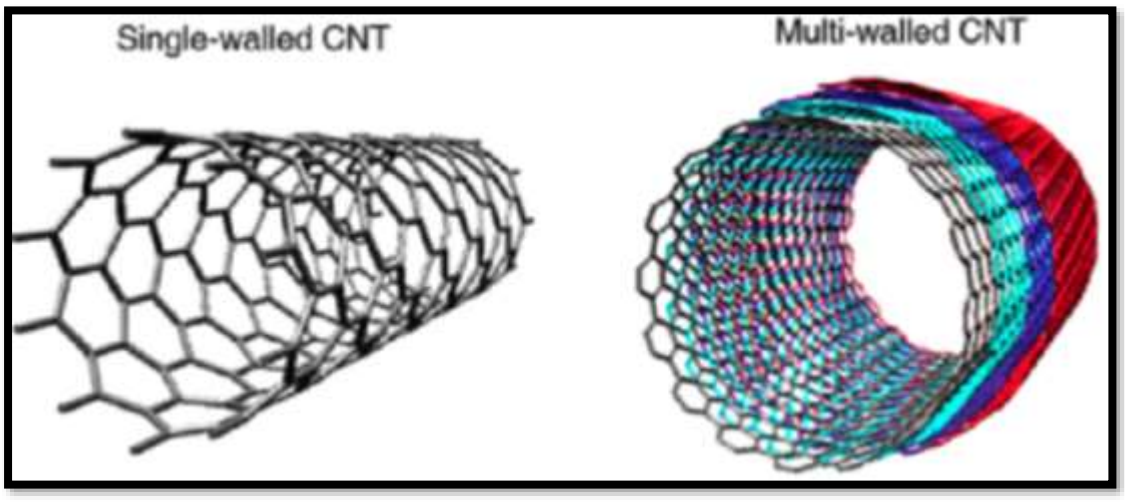

Fig. (1.4) The Schematic structure of SWCNT and MWCNT[35].

Table (1.1): a comparison between (SWCNT) and (MWCNT)

No.	SWCNT	MWCNT
1	Single layer of graphene	Multiple layer of graphene
2	Bulk synthesis is difficult	Bulk synthesis is easy
3	Purity is poor	Purity is high
4	Easily twisted	Difficult twisted
5	Less accumulation in body	Less accumulation in body
6	More defection during functionalization	Less defection, but difficult improve
7	Catalyst required for synthesis	Can be produce without Catalyst
8	Easy characterization and evaluation	Difficult characterization and evaluation

1.11 Literature Review:

- ***Somayeh et al. (2010),*** studied of the gas sensing property of polymethyl methacrylate for carbon nanotubes to detect acetone vapor at room temperature because it is an active ingredient. By the method of spin coating, polymeric films were formed. It is then using a suspension drop method of carbon nanotubes in acetone onto PMMA membranes. They were analysed by scanning electron microscope, Transmission electron microscopy, and Raman spectroscopy. The principle of gas sensing is used as the electrical resistance variation of the film after exposure to polar and non-polar gases. As for the samples, the results of the experiment indicated that there is a chemical reversibility and selectivity towards polar gases, especially acetone vapor [36].

- ***Payam Molla-Abbasi et al. (2011)***, studied the effect of PMMA doping by MWCNTs polymer on the sensitivity of porous sensing films synthesis by a non-solvent induced dry cast phase separation technique. It has been found the rate was five times higher than the responses of the dense membranes when the thickness was fixed. A higher response to a set of organic vapors has been observed for the functionalized carbon nanotube PMMA porous composite sensors. Their response was 10 times higher than that of similar sensors with no carbon [37].
- ***Hong-Di Zhang et al. (2014),*** indicate that the mechanism of manufacturing PMMA fibers was studied using electrospinning method, and then polyaniline nanoparticles appeared on the surface of parallel PMMA fibers through On-site polymerization of the solution. The structure and composition of PANI/PMMA compliant composite fibers were analyzed by Raman spectrometry and scanning electron microscopy. The gas sensing properties of composite fibers are tested at very low ammonia concentrations at standard temperature. Results have been obtained Indicates when the arranged fibers are exposed to ammonia vapor; they have a very high sensitivity and a very fast response at a rate of 1-30 ppm. [38]**.**
- ***Nanda GopalSahoo et al. (2016)***, It has effective mechanical, electrical and magnetic properties exhibited by carbon nanotubes (CNTs) as well as their it's nanometer diameter makes it a good reinforcing agent for polymer composites that have high strength and aspect ratio. However, because carbon nanotubes always compose fixed bundles because of van der Waals interactions it is difficult to characterize and align a polymer matrix. The biggest problems in preparing carbon nanotube booster vehicles lie in the effective dispersion of carbon nanotubes in a polymer

matrix, and the dispersion, in carbon nanotubes in the matrix the control is evaluated [39].

- ***Bharti et al. (2017),*** indicate that the influence of nanotubes on the set of electrical and optical features of polymathic methacrylate for both multi-walled carbonate as well as fast heavy ionic radiation was studied. The self-sustaining films of non-conducting PMMA and Multi-walled carbon nanotubes PMMA nanocomposites were irradiated under vacuum with 50 MeV Lithium and 80 MeV Carbon at 1 × 10 ionic impacts. The results showed that finding the peak light (PL) band in Spectra of Raman [40].
- ***Subhendu Bhandari et al. (2018)***, studied various carbon fillers such as carbon black, (single and multi) walled carbon nanotubes, graphene, fullerene, etc. widely for potential application in sensors. There was a major role for matrix filler composition in the sensing activities. Apart from the original fillings, he also explained that chemical modifications improved the performance of the sensor in many cases. Furthermore, a mixed mixture of two fillings can be used firmly, and in some cases can be show a synergistically enhanced sensing behavior. Achieving an illness level of pressure sensing at a low filler load is challenging. Likewise, some factors are of paramount importance in improving the Performance and effectiveness of temperature or gas sensors such as further improvement of the temperature sensing range and the selectivity of vapors or gases there [41].
- **Shujahadeen B. Aziza et al. (2019)** , studied the synthesis of polymer composites with an amorphous structure which is of great interest for optoelectronic device applications. Specific techniques such as solution casting technology were used to prepare films from PMMA/CNDs. Fourier transform showed the results of infrared spectroscopy of the

complexity incident between PMMA and CNDs. Whereas, X-ray diffraction analysis showed optimization in the amorphous phase of PMMA with the addition of CNDs. By means of field emission electron microscopy, the surface morphology of the films has been examined of non-porous PMMA/CNDs films was shown to be dominated by broadband around 480 nm from photoluminescence (PL) spectroscopy study[42].

- ***Mergen, Ömer Bahadır et al. (2020)***, dealt with the preparation of poly (methyl methacrylate)/multi-walled carbon nanotube (MWCNT) composite thin films by simple and efficient solution mixing and ultrasonic method and the electrical, optical, and mechanical characterizations. Scattered light intensity (I_{SC}), tensile modulus (E), and surface conductivity (a) of these composites have increased with the addition of MWCNT into the composite. The optical, mechanical and electrical properties of poly (methyl methacrylate)/MWCNT composites were increased with increasing MWCNT content until it reaches to 10 wt%. However, above u ¼ 10 wt%, the mechanical properties of the composites were decreased due to the aggregation of MWCNTs, while the toughness does not show a significant change until u ¼ 10 wt% MWCNT content, whereas it was decreased above this value.[43].
- ***Qazi, et al. (2021)***, indicate that partially degradable polymeric nanocomposites poly (3-hydroxybutyrate) (PHB multi-walled carbon nanotubes poly (methyl methacrylate as well as non-biodegradable nanocomposites (MWCNTs/PMMA) synthesized, thermoelectric and thermoelectric. Multi-walled carbon nanotubes have been under preparation to ensure the Active dispersion in the grafted PHB polymeric matrix adopting the “grafting” method. PMMA/PHB mixing system through mixing solution. Efficient thermal features shown in all the nanocomposites of the PHB/f-MWCNTs/PMMA mix systems. Higher

frequency amplitude values are noticed in nanocomposites having F-MWCNTs and g-MWCNTs in comparison with to nanocomposites having p-MWCNTs and a-MWCNTs because of their very good reactivity and excellent dispersion in the polymer mixtures. Ammonia sensor data analysis has shown that the PHB/g-MWCNTs/PMMA nanocomposites has good sensitivity and had good reproducibility and consistent responses. The calculated limits of detection is 0.129 ppm for PHB/g-MWCNTs/PMMA, in comparison with the limits for all other nanocomposites over 40 ppm [44].

- ***Lamis and Mohammed (2022)***, prepared the thin films of poly (methyl methacrylate) [PMMA] by spinning coating process. In addition, study the effect of adding concertation PMMA. Changes in optical parameters have been measured. The outcomes has shown witnessed the transmittance values with all PMMA concentration ratios. The values of reflectance increased when the concentration ratio has increased; beside that, the outcomes have witnessed decreasing in the energy gap for allowed direct transition as the concentration ratio increases the PMMA [45].

1.12 Aims and Objectives:

This study aims to conduct basic research on developing new research to prepare PMMA-CNT (nanocomposite) thin film that can be extremely used in gas sensors. The aims of the current study are as follows:

I. Analysis of structural and optical properties of prepared (PMMA-MWCNTs) thin films by spin coating technique deposited on glass substrates and analysis of the impact of MWCNTs doping on the structural and optical properties of films by crystallite size, surface roughness, optical energy gap.

II. Investigating the optimization conditions for prepared (PMMA/ MWCNTs) gas sensors for poisonous gas like NH3 and NO2.

1.13 Thesis Scopes:

This thesis is divided into four chapters, chapter one presents an introduction as well as a literature review related to the work. The study objectives are listed at the end of the chapter. In chapter two, a brief description of the theoretical background of our study is provided accompanied by a description of the characterization tools used to conduct this study. A complete description of the materials, tools and methods are presented in chapter three. Chapter four is devoted to presenting and discussing the results we obtained.

Chapter Two

Theoretical Part

2.1 Introduction:

This chapter contains all the mathematical relationships used, the physical concepts, the laws used, and the materials and methods used, also describes the theoretical part so that the results obtained are explained.

2.2 Spin Coating Process Theory:

2.2.1 Background and Method:

The spin coating process is known to be simple for a relatively quick deposit of light coating on glass substrates. It is done using a rotatable fixture (usually a vacuum is used to install the substrate in place) where the substrate to be used is fixed to cover it and the coating solution is distributed over the surface; then a very uniform coating of the selected material is left on the surface of the substrate as a result of the spinning action in spreading the solution. In the past, the coating process was rotating, it has been extensively studied and much is known about the factors that control the final thickness and coating deposition of the sediment that produces [46,47]. The current review of spin coating emphasizes the related features of Sol-Gel solution derived, particularly concerning coating defect identification and defect prevention[48]. Summary of fluid flow physics and solvent evaporation determines the common conditions for most spin coating protocols will be reported. These defects often form when these boundary conditions are responsible. The next section sometimes defects appear when making Sol-Gel paints and then cover a combination of these defects. Whereas, ways are suggested to prevent these defects from forming and appearing.

To generate thin and homogeneous organic films from solutions we resort to spin coating, as it is a quick and easy method. Spin coating is commonly used as a procedure for applying thin, uniform films on flat substrates. After a specified period, an excess amount of the solution is

applied to the substrate, to diffuse the liquid which is then circulated at high speed by centrifugal force [49]. In the early stages spin coating, by centrifugal force the dilution rate is much greater than the evaporation rate. After cleavage, film thinning is due to evaporation and occurs constantly. The point at which the centrifugal thinning rate is the same as that caused by evaporation is the transition point between evaporation and evaporation. Figure (2.1) illustrates the stages of spin coating; the thickness of the film at each different transition point is illustrated. Drying time is the time after the transition point is reached. Due to the evaporation of the solvent, the liquid film becomes supersaturated. A solid film is formed on the substrate after the evaporation of the solvent is completed [50].

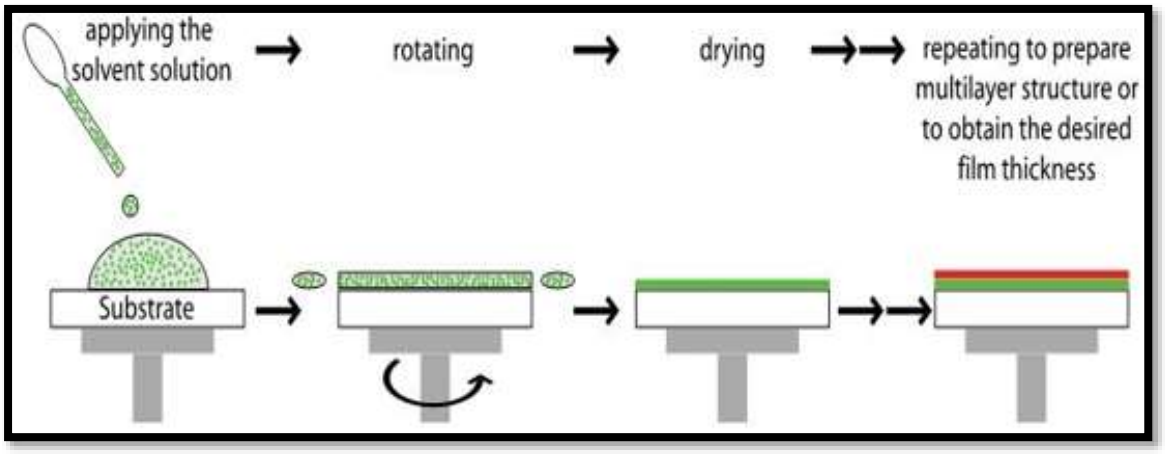

Fig. (2.1) shows the schematic figure of spin-coating[50].

2.3 Structural Properties:

2.3.1 Fourier Transform Infrared:

To obtain the infrared absorption and emission spectrum, we use FTIR technology, optical conductivity, or Raman scattering of a liquid or solid, or gaseous substance. Simultaneously in a wide range of the spectral range, the spectrometer collects spectral data. A scan range (500-4000) cm^{-1} and a solution (1 cm^{-1}) is usually used. FTIR is used to determine the quality of chemical bonding in samples and the formation of a new

compound. Some infrared radiation is absorbed and transmitted by the sample when it is irradiated with infrared (IR) light.

The spectrum obtained represents the fingerprint of the sample. By FTIR analysis, the quality of components in composite samples and in the identification of unknown substances is determined, so it is a powerful tool [51].

2.3.2 Atomic Force Microscope (AFM):

Atomic Force Microscope is one of the types that is characterized by its high accuracy of microscopy sensor, with a very high resolution through which a surface can be viewed where this resolution is (100 μm to less than 1μm) [52]. AFM is used to obtain information about surface morphology through film surface imaging, Such as uniformity and distribution of grain or defect such as insulation or action that forms on any surface without damaging the surface. Many materials are identified by this technology, such as polymers, metals, semiconductors and composites [53]. Figure (2.2) A schematic diagram of an atomic force microscope is shown**.**

Atomic absorption spectroscopy is an analytical technique that measures the concentration of elements. A sensor can measure parts per billion. Technology takes advantage of the wavelengths of light, especially those absorbed by an element, depending on the amount of light absorbed at a specific wavelength, the element that corresponds to the known properties of the element we want to test is detected. An atomic absorption spectrum has many uses in the fields of chemistry to detect metal concentrations.

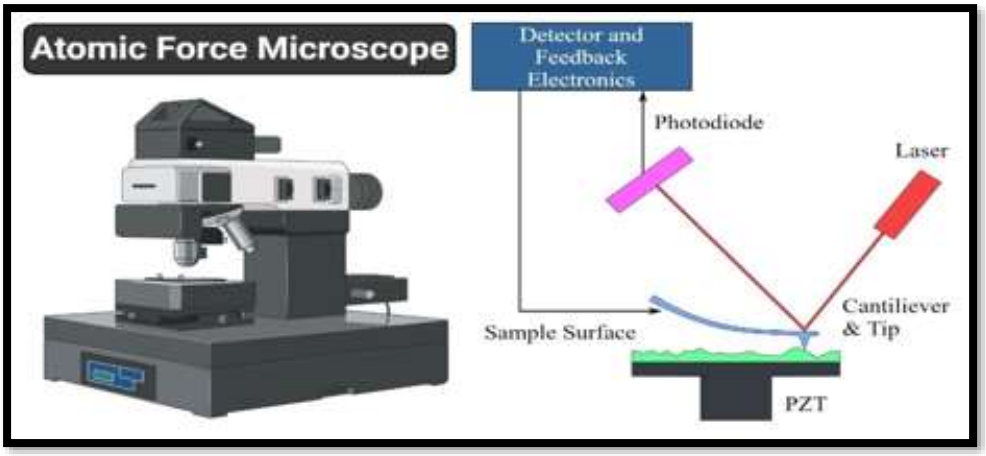

Fig. (2.2) The diagram for atomic forces microscope [40].

2.3.3 The X-Ray diffraction (XRD):

For preferred crystal orientation, using X-ray diffraction (XRD) is a widely used temporary methods and determination of lattice parameters.

When an X-ray beam is a monochromatic event in the crystal section, useful diffraction (or interference) occurs for parallel planes of atoms with spacing (d) between the Bragg planes if the law is fulfilled[54].

XRD is a nondestructive test that can be used to identify crystals, stages, and the determination of structural features and phases. XRD samples were prepared by placing the powder directly on the glass slide. Measurements of 2θ from 20° to 80° were considered and the XRD data was analyzed for peak position and location [55].

$$2d_{(hkl)} \sin\theta = n\lambda \qquad (2.1)$$

As :

d: the distance between the two sides' surface.

λ: The length of the wave of the incident ray (1.54 Å).

n: integer (represents order diffractions).

θ: Angle of incidence and reflection of the package X-rays beam and the surface.

hkl: millers coefficient

The Bragg scientist is able to tell the X-ray diffraction pattern of a crystal after it fell on it by superimposing a simple pattern of crystal structure. This replica provides for different levels of crystal atoms can reflect X-rays. Figure (2.3) the final version shows how Bragg found this law, shown in this image.

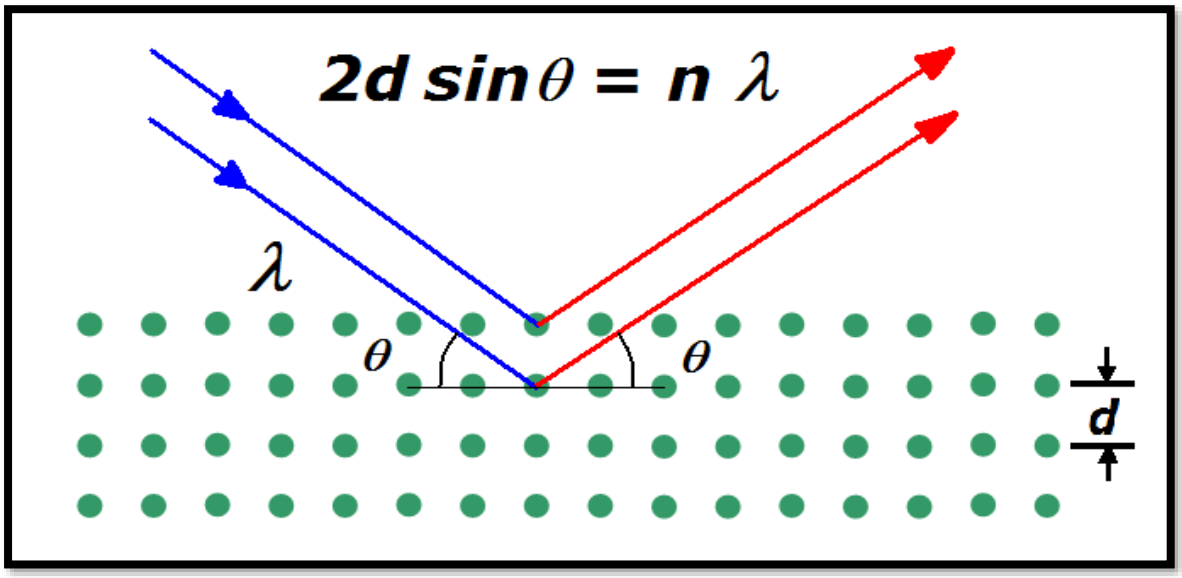

Fig. (2.3) The Bragg reflection [56].

2.4 Optical Properties:

The optical properties of materials are properties that focus on the interaction between electromagnetic radiation or light with on object, which include polarization, absorption, reflection, and scattering effects[43].

2.4.1 Absorbance (A):

Absorption could be illustrated as the ratio of the absorbed light intensities (I_a) by materials with the incident intensities of light (I_o)[44].

$$A = \log \frac{Ia}{Io} \qquad (2.2)$$

2.4.2 Transmittance (T):

It could be acquired through the ratio of the intensities of the ray transmittance (I_T) within the films to the intensities of the incident rays (I_o) on it as [41]:

$$T = \frac{I_T}{I_o} \qquad (2.3)$$

Beside that, It could be found that the transmittance as an operation of the wavelength through the exponential relation for both absorbance and transmittance [45]:

$$A = \log\left(\frac{1}{T}\right) \qquad (2.4)$$

2.4.3 Reflectance (R)

Reflectance could be acquired by the absorbance and transmittance spectrum based on the laws of transforming energy through the following[46]:

$$R + T + A = 1 \qquad (2.5)$$

2.4.4 Absorption Coefficient (α)

This could be illustrated as the relative rate of decreasing the light intensities (I) with the propagation paths. According to Beer Lambert low[47]:

$$\alpha = \frac{1}{I}\frac{d[I]}{dt} \qquad (2.6)$$

Where

I: represents the intensities of light in (W/cm^2)

t: indicates the thickness of thin film in (cm).

α can be given by [54]:

$$\alpha = \frac{2.303\ .A}{t} \qquad (2.7)$$

, α represents a good function of the wavelength or photon energy. Photon energy is given by[47]:

$$E = h\upsilon \qquad (2.8)$$

as:

υ: indicates the frequency in (Hz.)

h: represents Plank constant (6.625×10^{-34} J.s).

2.4.5 Extinction Coefficient (k_o):

Extinction Coefficient indicates the imaginative side of the complex refractive index (n*)[48]:

$$n^* = n - ik_o \qquad (2.9)$$

as :

n : indicates the real part of refractive index , equal (c/v).

c : indicates velocity of light in space

v : represents the velocity of light in thin films

n*: represents the complex refractive index that is dependent on the materials type, crystal structures (grain size), crystal defect, stress in the crystal and extinction coefficient (k_o), is represented as [48]:

$$k_o = \frac{\alpha\,\lambda}{4\,\pi} \qquad (2.10)$$

as:

λ : represents the wavelength of incident photon rays.

α : indicates absorption coefficient.

2.4.6 Refractive Index (n):

It could be illustrated as the ratio between velocities of light in vacuum (c), to their velocities within the materials. The values of refractive index (n) are measured statistically according to the reflectance and extinction coefficient (k_o) as in [41]:

$$R = \frac{(n-1)^2 + k_o^2}{(n+1)^2 + k_o^2} \qquad (2.11)$$

(n) could be represented as [41]:

$$n = \left[\left(\frac{1+R}{1-R}\right)^2 - (k_o^2 + 1)\right]^{\frac{1}{2}} + \frac{1+R}{1-R} \qquad (2.12)$$

2.4.7 Dielectric Constant:

If the light incidents on the atoms o the materials, there is a reaction between incident radiations and the charge of the materials. This in turn would polarize the charges of the materials[41]:

$$\varepsilon = \varepsilon_1 - i\varepsilon_2 \qquad (2.13)$$

as :

ε_1 : indicates the real parts of the complex dielectric constants,

ε_2 : represents the imaginary its parts. The following formulas could be used to calculate the dielectric constants[41]:

$$\varepsilon_1 = n_o^2 - k_o^2 \qquad (2.14)$$

$$\varepsilon_2 = 2\, n_o\, k_o \qquad (2.15)$$

2.4.8 The major Absorption Edge

It indicates the band-to-band or to excitation transition (i.e. to excite electrons from the valence bands to the conduction bands), manifesting itself through rising the absorption rapidly. This could be employed in determining the energy gaps of the semiconductor. Absorption regions could be divided into: [49].

a. High Absorption Region

Figure (2.4, A) illustrates this region. (α) is higher or equals (10^4 cm^{-1}). The magnitude of forbidden optical energy gaps ($E_g^{opt.}$) could be presented.

b. Exponential Region:

Figure (2.4, B) illustrates this region. (α) equals ($1\ cm^{-1} < \alpha < 10^4\ cm^{-1}$). This indicates the transitions between the extended levels from the (V.B) to the local levels in the (C.B) and vice versa.

c. Low Absorption Region:

The value of (α) in this region is too small (α< 1 cm^{-1}). The transition happens in this region because of density of state in mobility gap resulted from the structural faults see Fig (2.4(C)).

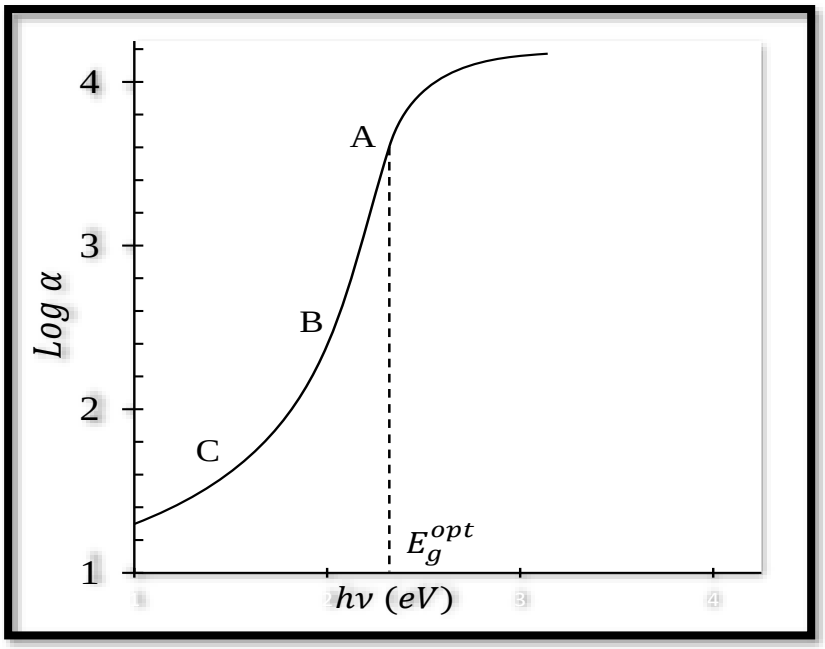

Fig. (2.4): The variation of absorption edge with absorption regions [57].

2.4.9 Electronic Transitions:

The absorption of radiation, that leads to electronic transition between the valence and conduction bands, is split into direct and indirect transitions see Fig. (2.5) [49].

The direct transition takes place in semiconductors while the bottom of (C.B) is directly over the top of (V.B). This indicates that they have the identical value of wave vector, i.e. (ΔK=0) in this case the absorption appears if ($h\upsilon=E_g^{opt.}$). This type of transition is needed for the Law's of conservation of energy and momentum. such direct transitions have two types[49].

a. Direct Allowed Transitions:

The transition takes place from the top points in the (V.B) and the bottom point in the (C.B) see Fig. (2.5.a).

b. Direct Forbidden Transitions:

It takes place close to the highest point of (V.B) and the lowest point of (C.B) [51], see Fig. (2.5.b).

The value of (α) of this type is achieved as follows:

$$(\alpha\, h\upsilon) = B\,(h\upsilon - E_g^{opt.})^r \qquad (2.16)$$

As :

$E_g^{opt.}$: represents energy gaps between direct transition.

B: indicates the constants depending on the kind of materials.

r: exponeat constant, its value depends on the sort of transitions:

r =1/2 for the allowed direct transition.

r =3/2 for the forbidden direct transition.

Concerning the indirect transitions bottom of (C.B) should not be above the top of (V.B), in (E-K) curve. The electron transited from (V.B) to (C.B) is not perpendicular as the value of the wave vectors of electrons before and after the transition is not equal ($\Delta K \neq 0$). such transitions take place with the aid of particles known as "Phonon", for conservations of the energy and momentum law. Two types of indirect transitions that are represented in [51]:

c. Allowed Indirect Transitions:

They take place between the highest point of (V.B) and the lowest one of (C.B). it is available in the difference region of (K-space) see Fig. (2.5.c).

d. Forbidden Indirect Transitions:

They take place between the closest point near the top of (V.B) and close point in the lowest part of (C.B) [58], see Fig (2.5.d). Its absorption coefficient with a photon absorption is represented as:

$$\alpha\, h\upsilon = B\,(h\upsilon - E_g^{opt.} \pm E_{ph.})^r \qquad (2.17)$$

as:

$E_{ph.}$: represents the energy of the phonon, is (-) when phonon absorption, and (+) when photon emission.

r = 2 for the allowed indirect transition.

r = 3 for the forbidden indirect transition.

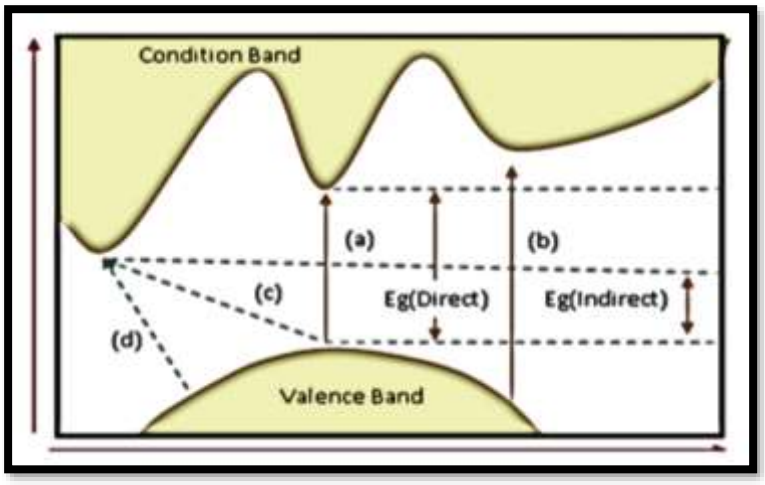

Fig. (2.5): The transition types[49].

(a) Allowed direct transition. **(c) Allowed indirect transition.**

(b) Forbidden direct transition. **(d) Forbidden indirect transition.**

2.5 Sensing Parameters:

2.5.1 Sensitivity:

Sensitivity can be defined as response of a gas sensor per unit change in the gas concentration. In the case of resistive gas sensors, it is defined as the relative change in resistance or conductivity of the thin film. It is the ratio of the change in the resistance (approximately to 90 %) of the thin film in air to the change in resistance in particular gas atmosphere. The sensitivity is given by the equation (2-18) for p-type semiconductor with oxidized gas and equation (2-19) for reduced gas [59]:

$$Sensitivity = \frac{\Delta R}{R_g} = \left|\frac{R_g - R_a}{R_g}\right| \times 100\% \qquad \cdots\cdots\cdots\cdots\cdots\cdots (2.18)$$

Where R_a resistance of the film sensor in air presence, R_g resistance of the film sensor in a gas presence. It can also clarify the sensitivity by the conductivity as:

$$Sensitivity = \frac{G_{gas}}{G_{air}} \quad \text{..... (2.19)}$$

Where (G_{air}) is the conductance of the sensor in dry air and (G_{gas}) is the conductance of the sensor in the air containing a given concentration of reducing gas.

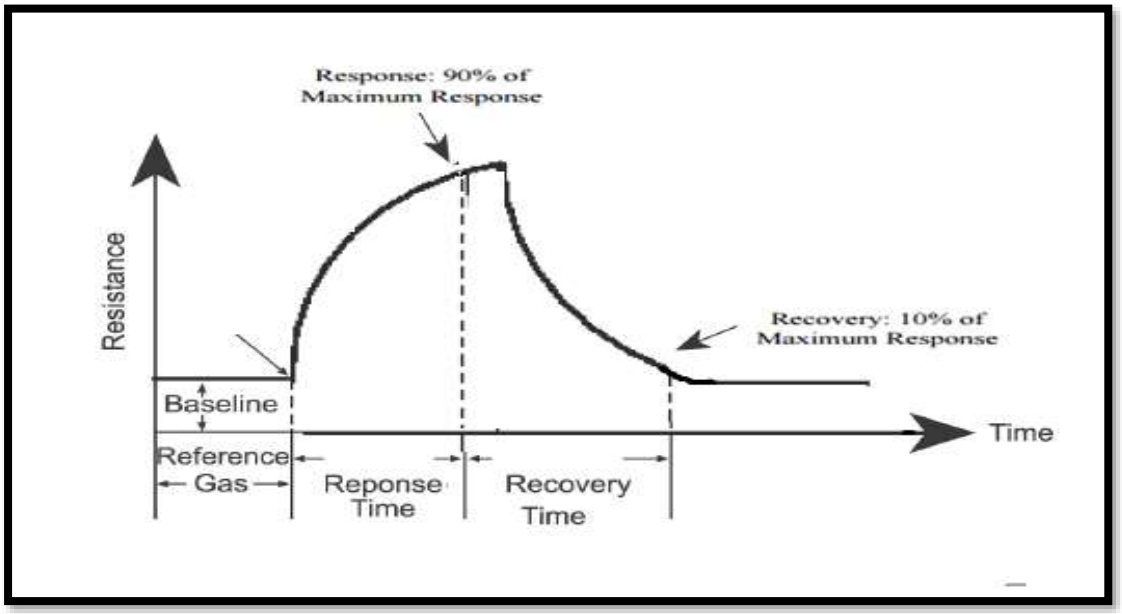

Fig. (2.6) A typical response curve of a conduct metric gas sensor [60].

2.6 Types of Sensors [61] :

1- Coustic Sensors used to calculate the wave capacity, phases, polarization and wave speed .

2- Electrical and magnetic sensors are used to detect the electromagnetic field, charge voltage, current, flow, conductivity, porosity, site control and location determination.

3- Mechanical sensors are used to detect location, speed, acceleration, momentum, momentum, speed, shape, roughness, viscosity, hardness, and material composition.

4- Optical sensors used in cameras and night vision systems.

5- Temperature and Flow Sensors are used in air conditioners and automatic systems.

6- Chemical and biological sensors used in biologic diagnosis systems.

7- Gas sensors are used to detect atmospheric gases.

Chapter three

Experimental Work

3.1 Introduction

This chapter gives a description of the procedures used in the preparation of PMMA/MWCNTs thin films and instruments for characteristic measurement were employed in this work as well as a study on the characteristic of films. Figure (3.1) shows a flow chart of the preparation PMMA/MWCNTs and study the physical properties of PMMA/MWCNTs thin film.

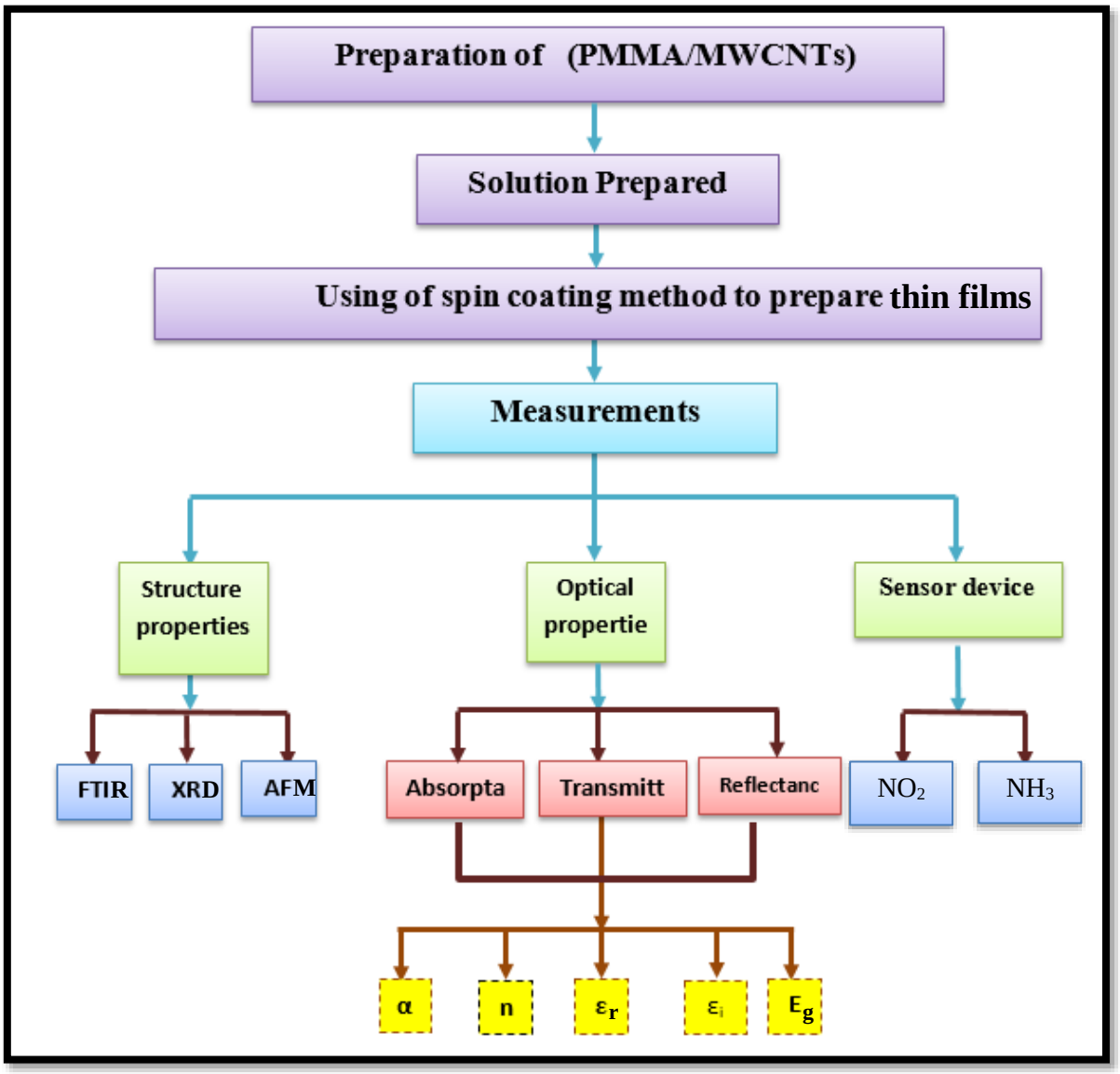

Fig. (3.1) flow chart of the preparation PMMA/MWCNTs.

3.2 Deposition of PMMA/MWCNTs Thin Films:

The deposition of thin films consists of:

3.2.1 Substrates Cleaning

The cleaning of the glass substrate can be summarized as follows:

a- We clean it by using detergent with water to remove dust and suspended fatty substances on the surface of the substrate, then wash it under tap water and gently rub it.

b- Put it in a clean container with distilled water and then put in a unit of ultrasound for 20 minutes.

c- Repeat the second step by replacing the distilled water and place the pure alcohol, which reacts with contamination such as grease and some oxides.

d- Finally, we dry the slides by shedding the air, and then wiping a spot of soft paper.

3.2.2 Formation of Polymer PMMA/ MWCNTs Thin Films by Spin Coating Technique:

The thin polymer films (PMMA / MWCNTs) are prepared from homogeneous polymer solution by spin coating procedure the composite films of the PMMA/ MWCNTs of a variety of the concentrations have been prepared by using the spin coating approach. Matrix material that has been utilized in the present work has been the polymethyl methacrylate, the PMMA solution were prepared by dissolving (0.1 mg) PMMA from (kareby bio company) in 10ml of chloroform. The solution then but on the magnetic stirrer for 30 s, multi.walled carbon nanotubes (MWCNTs) were added to the solution at different rate (1%,3%,5%). Finally, thin films have been prepared by spin coating rotation speed is 2000rpm and the rotation time is 10 s and films were dried at 60 °C. In this work influence of the concentration of polymer solution of the polymer film were studied.

3.3 Spin Coating

A photo resist spinner model 4000 (Electronic Micro Systems Ltd.) has been used to spin cast the thin films used in the current study. A droplet of the materials solution is placed using adjustable micro.syringe (10.100µl) onto a rotating substrate .The preparation of the samples have been carried out using VTC.100 spinner at the university of Babylon .The system consists of several parts arranged in such a way that it prepares different films and different concentrations by reducing or increasing the speed of rotation. Figure (3.2) shows the spin coating system.

Fig. (3.2) spin coating system with its control.

3.4 Structural and Morphological Measurement:

3.4.1 Fourier Transform Infrared (FTIR) Spectroscopy Test:

FTIR is a technique that uses the vibrational response of molecules when exposed to (IR) radiation. The use of IR spectroscopy comes from light with limited molecular vibrations interaction. Kinetic peculiarities of the polymer blend, dyes and nanocomposite material were examined utilizing the FTIR spectroscopy. The sample was put on a private FTIR holder so that the reconstructed beam is directed through the specimen and fixated on to the detector with the scanning range from (500-4000 cm^{-1}) and the resolution of (1 cm^{-1}). The output data is in the form of graphical diagram, in which the

x.axis represents the wave number; y.axis represents the transmission % in the IR region**.** FT.IR, by using Vertex 70 from broker company, Figure (3.5) shows that FT.IR Spectrophotometer present in the laboratory of the Department of chemistry, College of Science, University of Babylon**.**

Fig. (3.3) the FTIR instrument

3.4.2 X. Ray Diffraction Measurements:

In order to study the structural properties, the crystalline structure was analyzed with a SHIMADZU 6000 X. ray diffractometer system which records the intensity as a function of Bragg's angle and the result was obtained in the laboratory University of Kashan in the Islamic Republic of Iran. The X. ray diffraction measurement has been done according to the ASTM (American Society of Testing and Materials) cards. The source of radiation was Cuk_{α} with wavelength λ=1.5406Å, current 30mA and voltage 40 kV. The scanning angle 2θ is varied in the range of 20 – 80 degree and a speed of 4 deg/min as show in figure (3.4). The interpleader distance d_{hkl} for different planes was determined by using Bragg's law [55]:

$$n\lambda = 2d\sin\theta \qquad (3.1)$$

Where:

n: The reflection order.

θ: Bragg's angle.

XRD

Target : Cuk_{α}

Wavelength : 1.5406 Å

Current : 30 (mA)

Voltage : 40 (kV)

Range (2θ) : 20 to 80 degrees

Fig. (3.4) The (X-ray) diffraction system.

3.4.3 Atomic Force Microscopy (AFM):

The morphological properties of thin film in this work samples were studied. These were imaged by Atomic Force Microscopy (AFM) (CSPM.AA3000) device the result was obtained in the University of Kashan in the Islamic Republic of Iran and the device that been used in Figure (3.5). AFM images are obtained by the measurement of the force on a sharp tip (insulating or not) created by the proximity to the surface of the sample. This force is kept small and at constant level with a feedback mechanism. When the dimensional images of the surface of the samples are obtained.

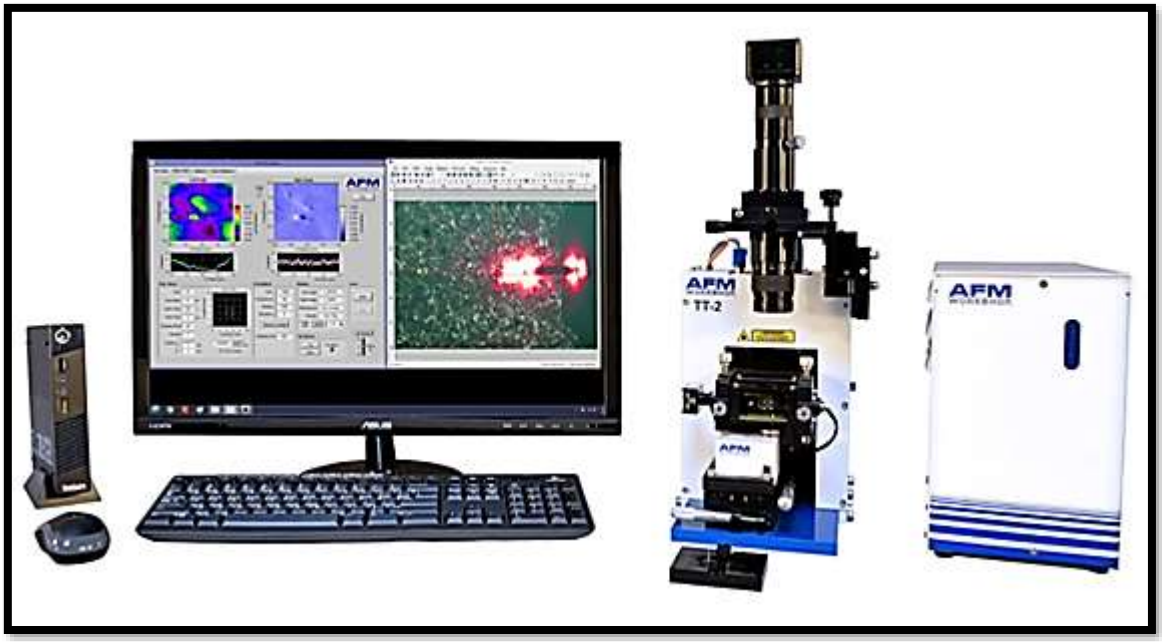

Fig. (3.5) The AFM device that used in these work

3.5 Optical Measurement:

3.5.1 UV. V is spectrophoto:

A single beam spectrophotometer UV.V is spectrometer (Lambda. LIMF 10), as show in figure (3.6), is used to record the optical absorption spectra of the PMMA /MWCNTs thin films at different concentration from MWCNTs within the wavelength range (200.800 nm). The optical properties of PMMA /MWCNTs are examined at room temperature in a quartz cell with (1 cm) optical path. The optical band gap was estimated graphically by applying the Tauc model; the band gap of the suspension with sharp fall off can be deduced from a plot of the squared absorption coefficient $(\alpha h\nu)^2$ versus photon energy ($h\nu$) by extrapolating the straight line of the plot to intersect the energy axis. This system is presented in the laboratory at the University of Babylon, College of Science, and Department of Physics.

Fig (3.6) The spectrophotometer using to measure optical properties.

3.6 Sensor System:

In the currents study, a gas sensor system is designed and constructed to operate in normal weather conditions and at laboratory temperatures and recording response data with the amount of gas flowing. The sensor device used in this study was found in department of physics, college of science, the University of Babylon

The sensor system consists of a glass flask with a capacity (500 ml) placed on a heater that can be controlled by a voltage cutter. The liquid to be heated is placed in the glass beaker and its temperature is gradually raised until it reaches the evaporation temperature. The glass beaker is connected to two glass tubes, each containing a valve that controls the passage of the gas, one of which is connected to a cylinder filled with nitrogen gas of 99% purity. The amount of nitrogen gas can be controlled by the gas flow meter. Nitrogen gas is an inert gas that does not affect the measurement process. It also drives the steam in the glass beaker to the sample to be measured. The other glass tube is connected to a room with a base for the sample to be measured in addition to four copper holders, two of which are used for the purpose of fixing the sample, the other two were used to connect the sample electrodes to a circle. Figure (3.7) shows the gas sensor system used in this study.

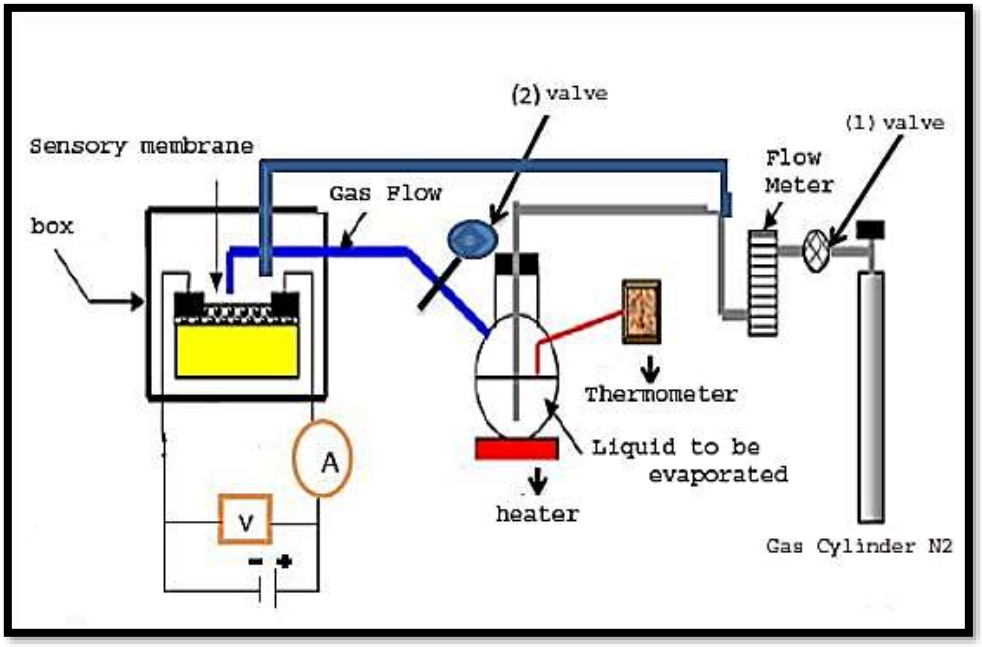

Fig. (3.7) The gas sensor system to measure sensitivity.

Chapter Four

Results and Discussion

4.1 Introduction:

This chapter presents the results and discussion of the experimental measurements, structural, morphological, optical of pure (PMMA) and doped with (MWCNTs) with different ratio of doping, as well as the effect of MWCNTs. doped on the efficiency of their sensitivity to gases.

4.2 Structural Properties for pure PMMA and doped MWCNTs thin films:

4.2.1 Fourier Transform Infrared Spectroscopy (FTIR):

FTIR spectra were recorded to understand the changes in the functional groups of pure PMMA due to the addition of CNTs The acquire spectra are shown as Figure (4.1) illustrates the pure PMMA and doping of PMMA polymer with (1, 3, 5) Wt.% MWCNTs the spectra were acquired in the range of 4000 to 500 cm^{-1}.

In case of pure PMMA, the methyl (–CH3) group bending vibration band is seen at 1436 cm^{-1}, while the band appeared ~1387 cm^{-1} is due to the methylene (–CH_2–)group deformation mode, while the band appeared ~3432 cm^{-1} for (O-H) . The band at around 1670 and 780 cm^{-1} are due to the stretching vibrations and out of plane bending vibration of the CO (carbonyl group). The spectrum for PMMA/CNTs nanocomposite shows absorption bands similar to that of pure PMMA. This is also evident from the reduction of the intensity of carbonyl group. Several bands between 1020–1300 cm^{-1} are known to be because of the ester group of syndiotactic PMMA that is in agreement with the reported data.

The band around 930 cm^{-1} is due to CH out of plane vibrations. Information about the wetting properties of such nanocomposite can be ascertained by measuring the contact angle of the prepared

specimen. The images acquired with DI water on the surface PMMA and CNTs loaded PMMA, wherein the effect is seen as improved wetting properties of the material. This improvement is a needed feature to increase the bioavailability of the nanocomposite material. Addition of 1 wt% CNTs leads to a reduced surface wetting which improves by addition of higher wt% of CNTs. This clearly indicates that the addition of CNTs changes the surface and reduces the surface tension of the specimen in regards to its wetting properties thereby affecting the biocompatibility with reference to pure PMMA.

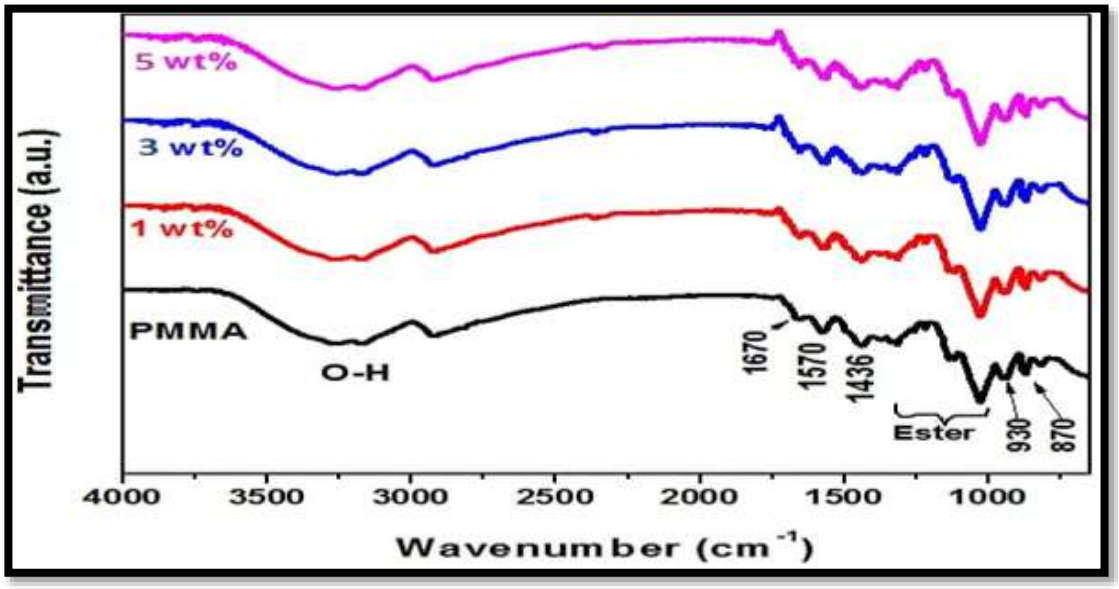

Fig. (4.1) The FTIR spectra of pure PMMA and doped polymer.

4.2.2 X-ray Diffraction Result for pure and doped thin films:

PMMA polymer doped with MWCNTs at different doping concentration for (1, 3 and 5wt %). The figure (4.2-4.5) .Show the XRD patterns of pure PMMA and doped polymers.

The figure (4.2) show PMMA polymers the diffraction peak of amorphous nature of PMMA polymer without adding any additive (MWCNTs).

At doping concentration of (1wt %) of WMCNTs diffraction peak located at 2θ = 34.4° as show in figure (4.3).as be seen increasing in the intensity of the peak with increasing doping concentration reported in the publication.

Similar Peaks have been noticed while adding MWCNTs to the PMMA matrix as illustrated in Figure (4.4). And many wide peak with a maximum angle at 2θ=14° , 34.4° and 40° could be activated through the absence of sharp shape peaks and the availability of broad Shaped ones .

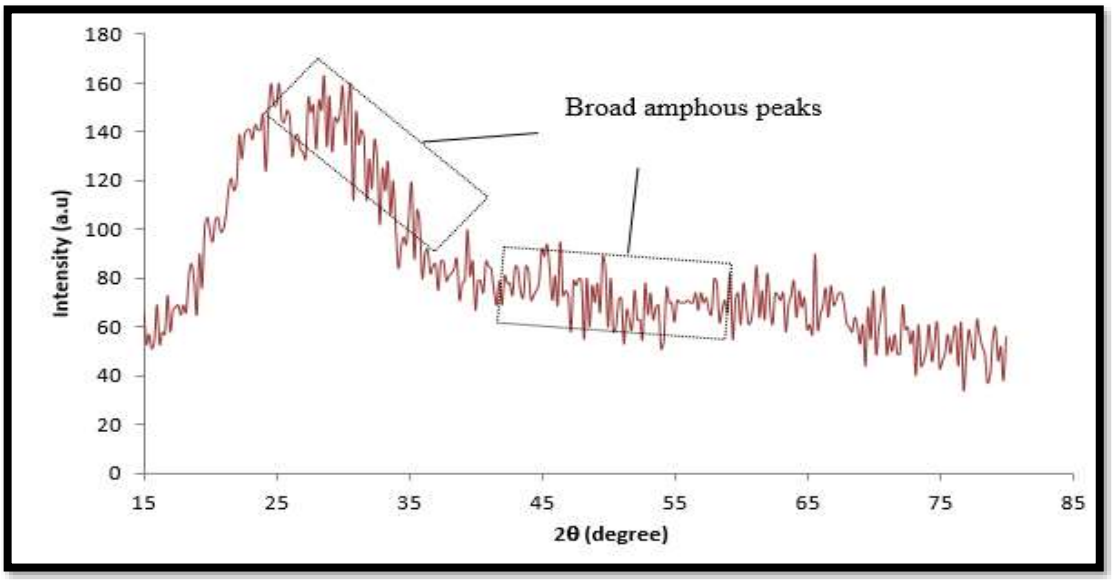

Fig. (4.2) The (XRD) pattern of pure PMMA.

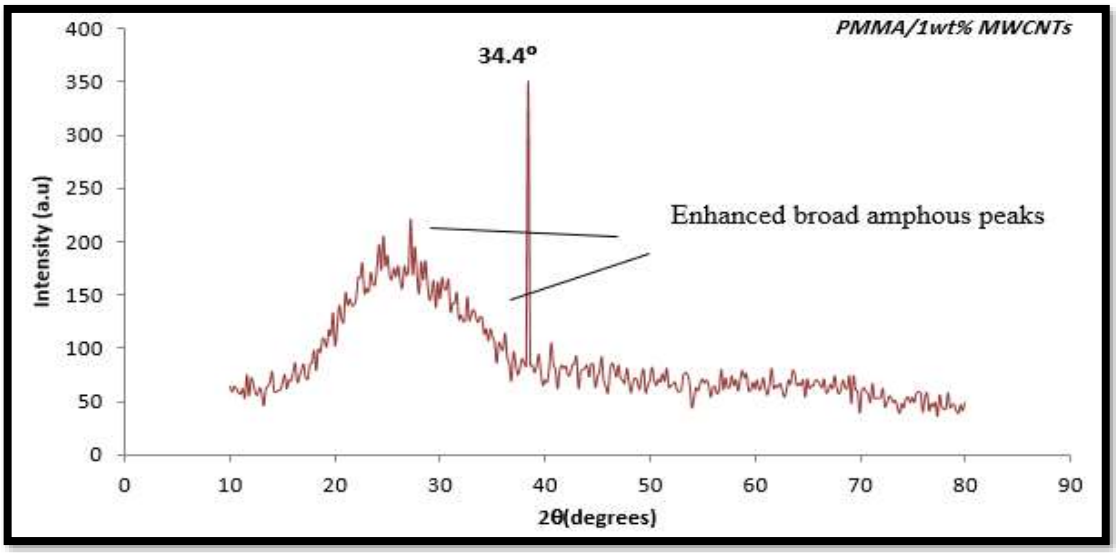

Fig. (4.3) The (XRD) pattern of PMMA .1wt% MWCNTs.

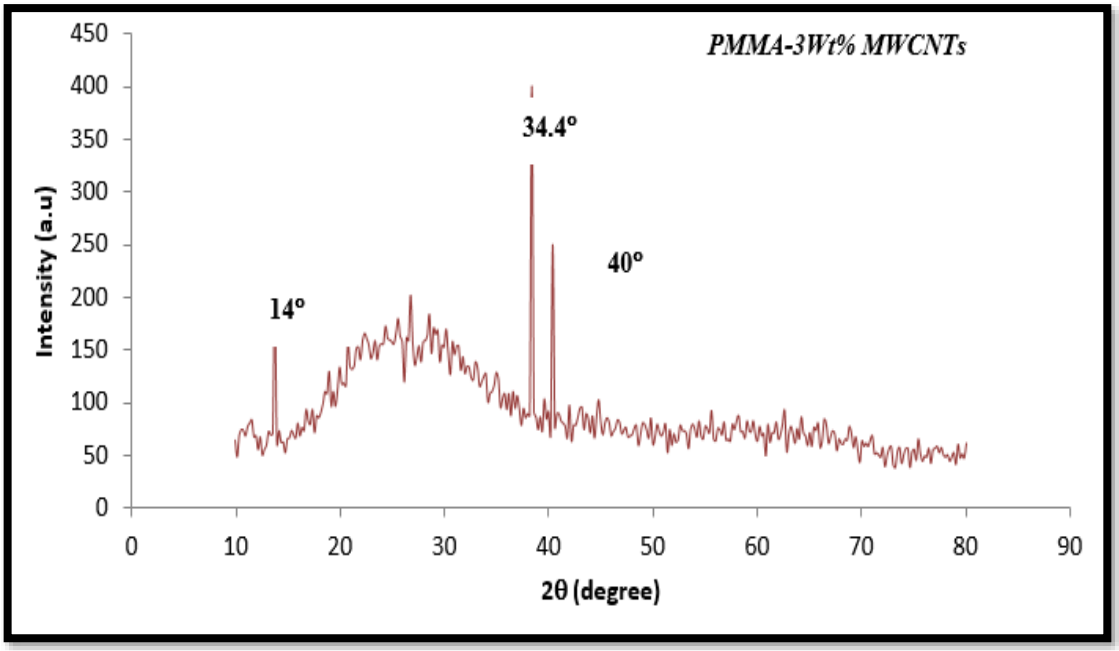

Fig. (4.4) The (XRD) pattern of PMMA.3 wt% MWCNTs.

In Figure (4.5), the decreased intensity of such peaks in the XRD-curves of the Nano-composite films indicates the availability of compatibly functioned Nano-composite systems, as well as compatible mix of polymers and MWCNTs. In addition, concerning the Nano-composite films, certain shifts in the diffraction peaks to less values are recorded. This implies the availability of some change in inter layer distance. Such behaviors imply that we do not have any covalent interaction between MWCNTs and PMMA .Besides that, this proves the homogeneity in the dispersions of CNTs in PMMA matrix. The collected outcomes agree with the ones of the retrieved studies also we can explain that decreases in the intensity of peaks for this value of doping (5wt%) that reason is and same worker attributes that to the presences of internal stresses by doping during spin coating , which can alter the energy balance between different crystal plane orientation because oxidation.

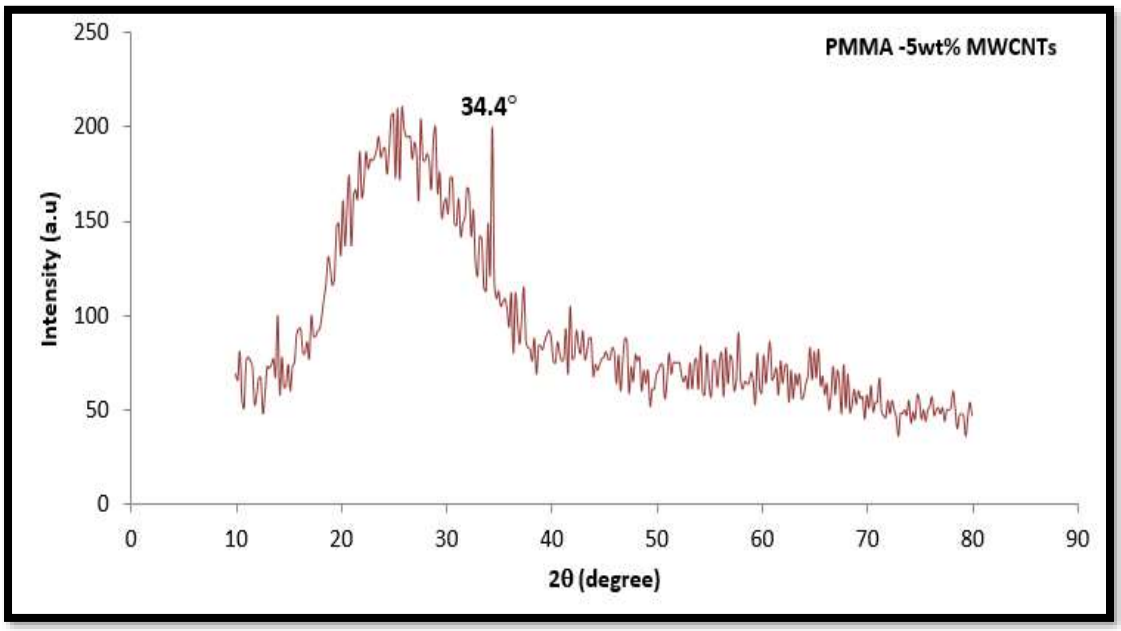

Fig. (4.5) The (XRD) pattern of PMMA .5wt% MWCNTs

4.2.3 Surface Morphology Atomic Force Macroscopic (AFM):

For the purpose of investigating PMMA concentration impact upon morphology, the films' topography has been determined with the use of the AFM approach, which has been illustrated in Fig (4.6a,b,c,d). AFM images have shown that all of the films are uniformed and there are no any significant differences between all of the concentrations. Average roughness Rms has been 75.72nm, 8.6nm, 10.11 nm and 7.47nm for 0, 1, 3, and 5 %from MWCNTS. Results have shown that RA is decreased with the increase of the concentration. Such decrease in surface roughness is a result of the viscosity of the solution with PMMA concentration increment. Table (4.1) explains the variability of Root Mean Square and grain size for PMMA at different doping concentrations of MWCNTs (1, 3,5 wt. %).

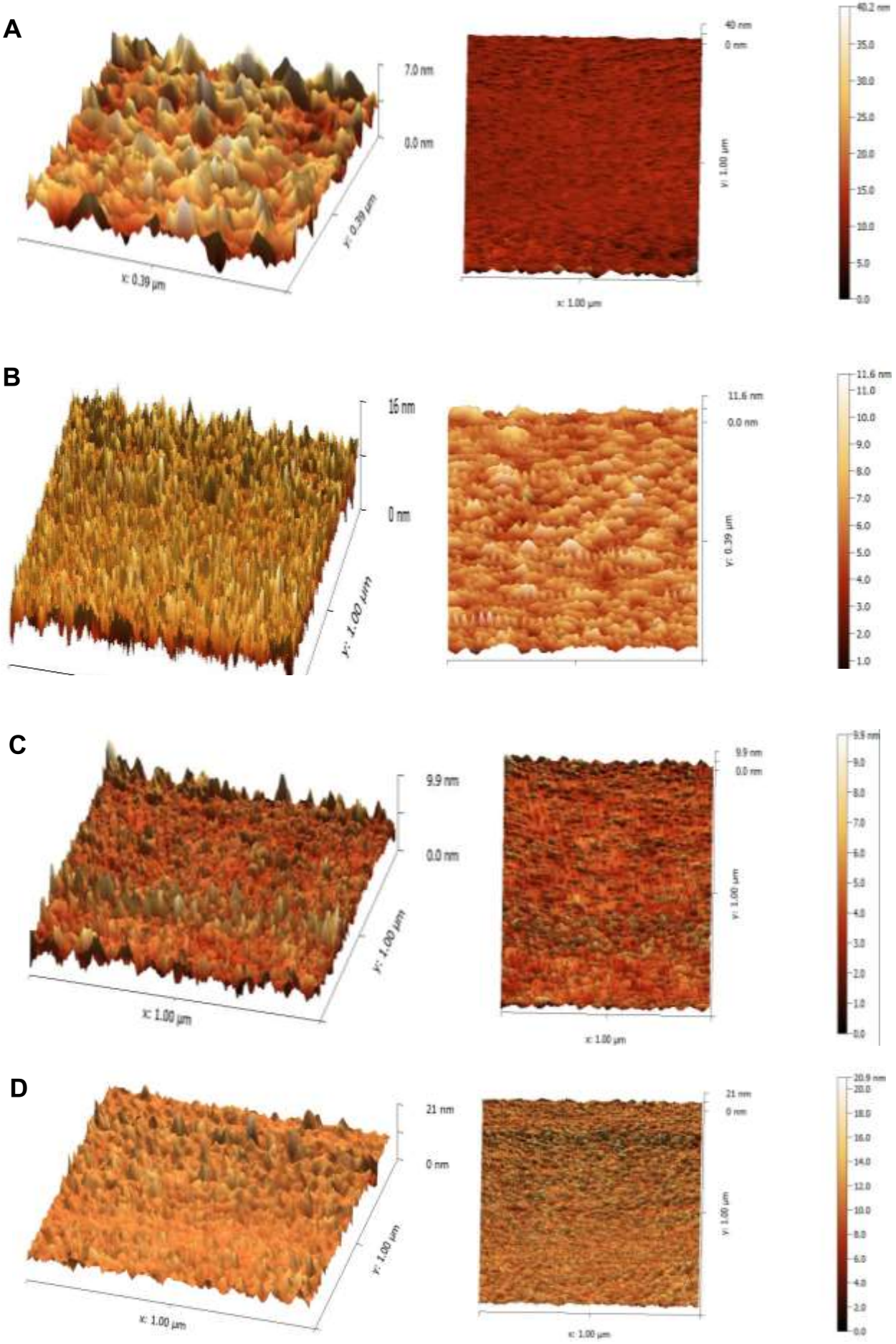

Fig. (4.6) The three - dimensional AFM images of the PMMA with different doping concetration (A,B,C,D).

Table (4.1) Variability in the root mean square and grain size for doped PMMA at different doping concentrations of MWCNTs (1, 3,5 wt. %).

Doping concentration	Root Mean Square (nm)	Roughness (nm)	Grain size (nm)
Pure PMMA	75.72	100	40
1 MWCNTs %	8.671	38	41
3 MWCNTs %	10.11	40	50
5 MWCNTs %	7.472	22	61

4.3 Optical Properties for pure and doped PMMA/MWCNTs thin films:

According to the energy conservative law and by referring to the quantum confinement, one can conclude what will happen if the incident wave length reacted with the outer shell electron. Hence, the electrons either absorb the photon or reflect the photon depending upon two parameters, frequency of the incident photon and the energy gap of the subjected material. Some variables will be discussed in the followings sections; they are related to the optical properties of PMMA and PMMA/ MWCNTs.

4.3.1 Transmittance spectra for pure and doped thin films:

The PMMA thin film transmittance spectra with a variety of the concentration levels have been measured at wave-length in a range of 200nm ~ 1000nm. Figure (4.7) illustrates spectra of transmittance for PMMA/MWCNTs films. It has been discovered that all of the samples have been almost transparent from UV until the region of the NIR. With the increase of the concentration, the transparency of the sample is decreased. This proves that all of the samples have PMMA main characteristic, which is high transparency.

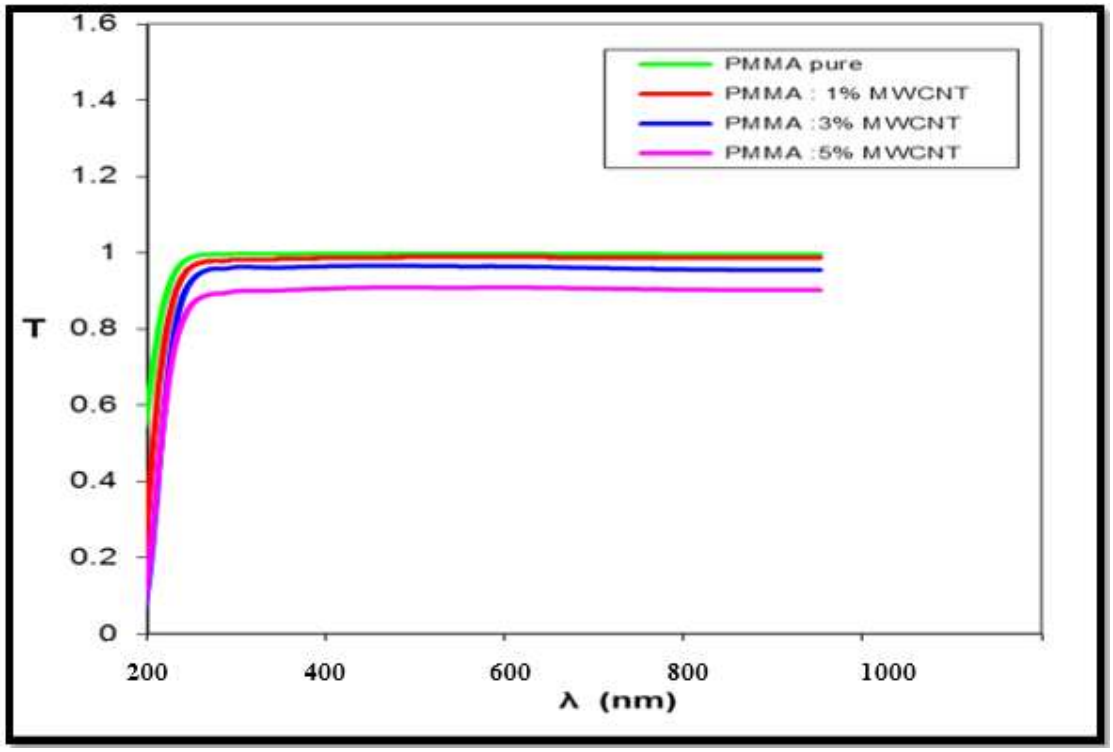

Fig. (4.7) The transmittance spectra of PMMA for different MWCNTs concentrations.

4.3.2 Absorption spectra for pure and doped thin films:

Concerning the absorbance (A) versus wavelength shown in figure (4.8) for the PMMA and the PMMA/MWCNTs thin films with different concentration, one can notice that the absorbance took high value near the absorption edge 220 nm for PMMA. Then, it decreases in the visible and near infrared regions. The same behavior occurs with composites except the absorption edge which is increased respectively with the additive increased.

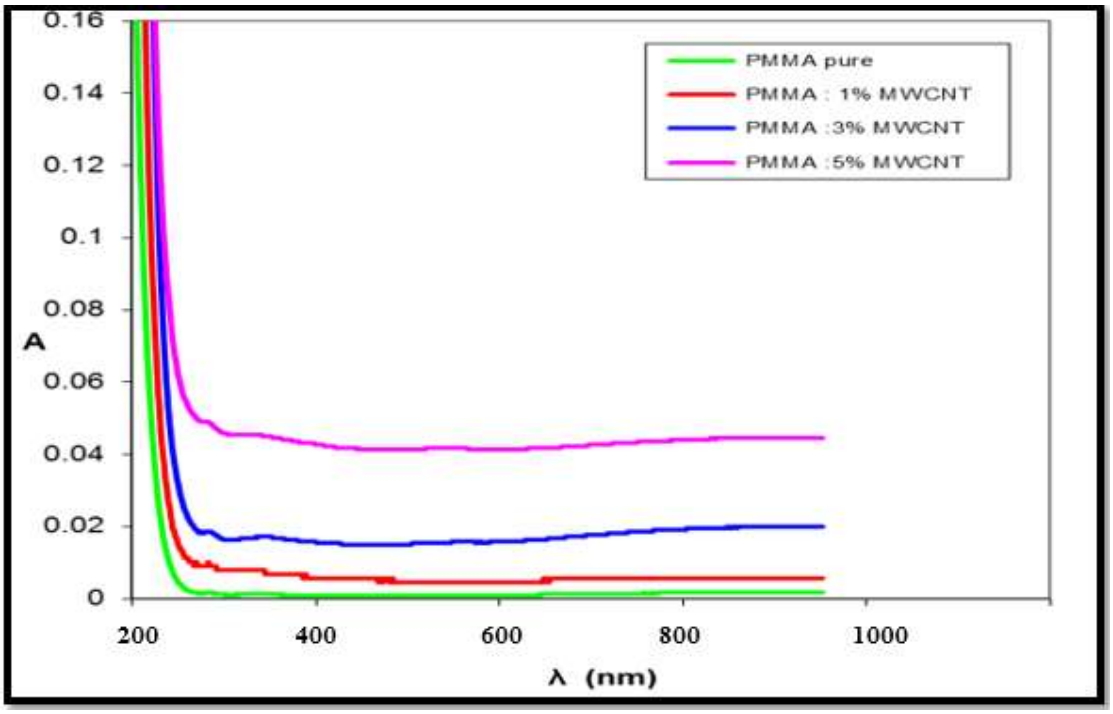

Fig. (4.8) The absorption spectra of PMMA for different MWCNTs concentrations.

4.3.3 Reflectance:

The reflectivity reflectance of PMMA pure and MWCNTs doped was calculated under the energy conservation act. Figure (4.9) represents the relationship that holds the reflectivity with wavelengths for pure (PMMA) and doped with variable ratio of MWCNTs. It could be observed from the illustration that the reflectivity increases with increasing wavelength for short wavelengths. For long wavelengths, reflectivity decreases with increasing wavelength and increasing deflection at short wavelengths less reflectivity and at long wavelengths becomes more reflective.

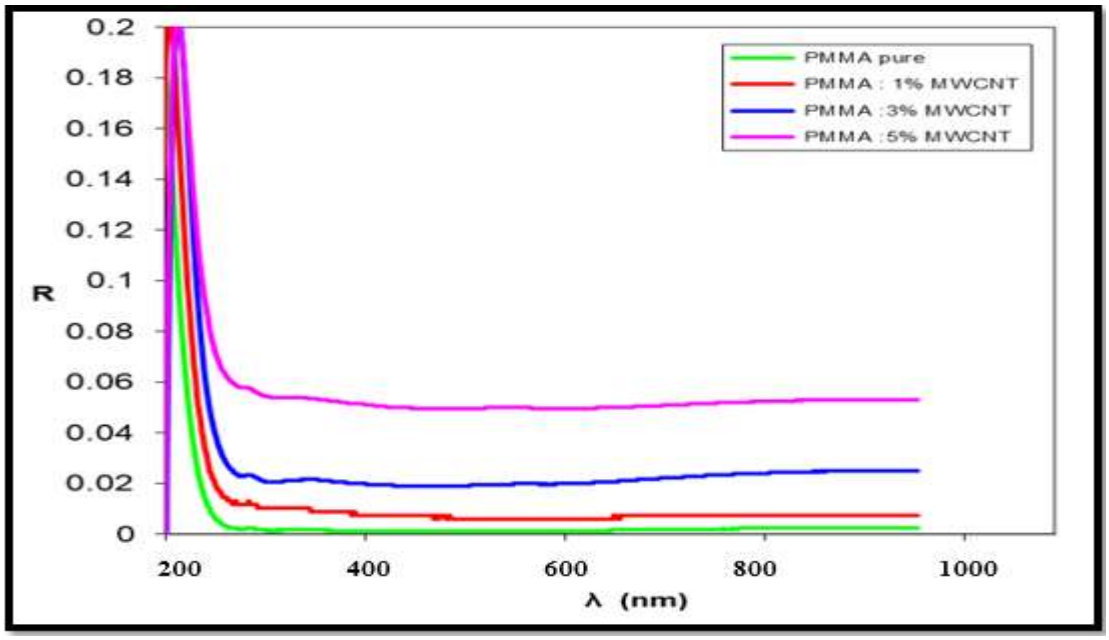

Fig. (4.9) The reflectance spectra of PMMA for different MWCNTs concentrations.

4.3.4 Absorption Coefficients:

The value of (α) for the thin films is seen to be higher than 10^4 cm^{-1} in the visible regions. This indicates that those films have direct optical energy gaps .The variability in the absorption coefficients (α) of (PMMA) films could be represented in the Figures (4.10 and 4.11) as a function of wavelength.

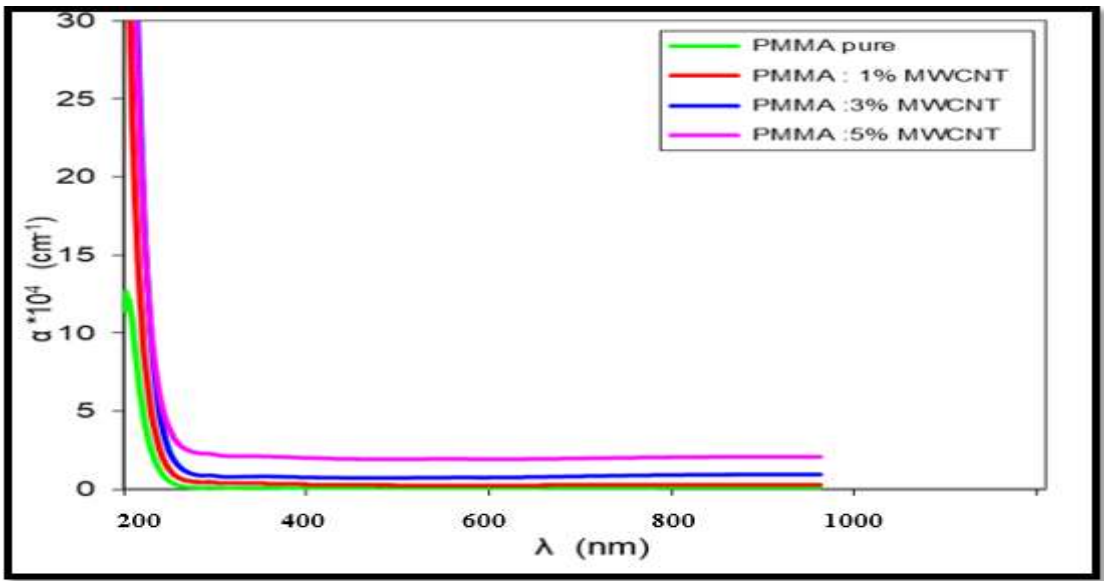

Fig. (4.10) The absorption coefficients as a function of wavelength for *PMMA/ MWCNTs*.

The figure shows that the absorption coefficient acts in a way that shows high similarity with the one of the absorbance spectrum, which is attributed to the nature of the relation that holds them as, represented in the equation

4.3.5 The direct optical band gap for pure and doped thin films:

The optical band gaps of the PMMA thin films at different doping concentrate from the MWCNTs. The UV.V is spectra of PMMA/MWCNTs Nano-composite thin films were evaluated as well with the aim of assessing the optical band gap according to Tauc'smodel. Just Tauc plots is evaluated according to the UV-Visible spectra from plot $(\alpha h\upsilon)2$ vs $(h\upsilon)$ for the PMMA/MWCNTs nano-composite thin films. Reported value of the optical band gap of MWCNTs can be varied from (3.8-3.5) eV with adding MWCNT to the PMMA, it is expected that PMMA shows lower value of optical band gap.

The analysis shows that the 0 wt.% MWCNTs gives the value of 3.8eV and the value was decreasing for the composition of 1 wt%, 3 wt% , 5 wt% MWCNTs. The optical band gap of all samples is summarized in Table (4.2) and shown in Fig. (4.11).

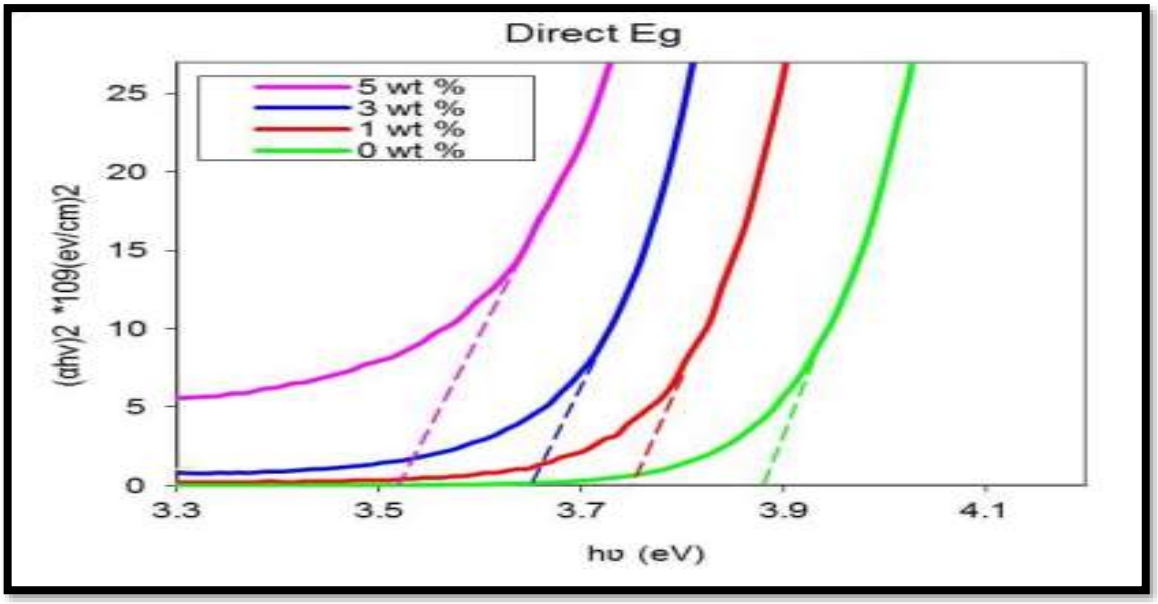

Fig. (4.11) The UV-visible spectra from plot $(\alpha h\upsilon)^2$ vs. $h\upsilon$ for PMMA/MWCNTs thin films.

It has been seen that with the increase of PMMA concentration there has been a decrease in the band gaps (Eg). Variations of the optical band gaps at different concentration of the PMMA could be a result of the optical scattering by grain boundaries. The decrease in the feature of the light absorption coefficient for the thin film that is prepared at a concentration of 25mg could be a result of defects in thin films that have gotten higher value as growth along the c-axis is reduced at high concentrations.

Table (4.2) show the band gap with doping content

Wt.% CNTs in PMMA/MWCNTs	Optical Band Gap (eV)
0wt%	3.88
1 wt%	3.75
3 wt%	3.65
5 wt%	3.52

4.3.6 Refractive index (n) for pure and doped thin films:

This represents one of the important parameters for the optical applications and materials. Which is why, there is an importance for the determination of the optical constants of films. The films' refractive index has been specified from the equation below [24.

$$n=\frac{1+R}{1-R}\sqrt{\frac{4R}{(1-R)^{2}-K^{2}}} \qquad (4.1)$$

R represents reflectance and k indicates the coefficient of extinction (k= $\alpha\lambda/4\pi$) where $\alpha$is the coefficient of the absorption. The $n$and k values of dependence of the wave-length, respectively, for all of the samples prior to and post being doped. As it is seen in figure (4.12), the n and k values are increased with the increasing of MWCNT doping concentration .

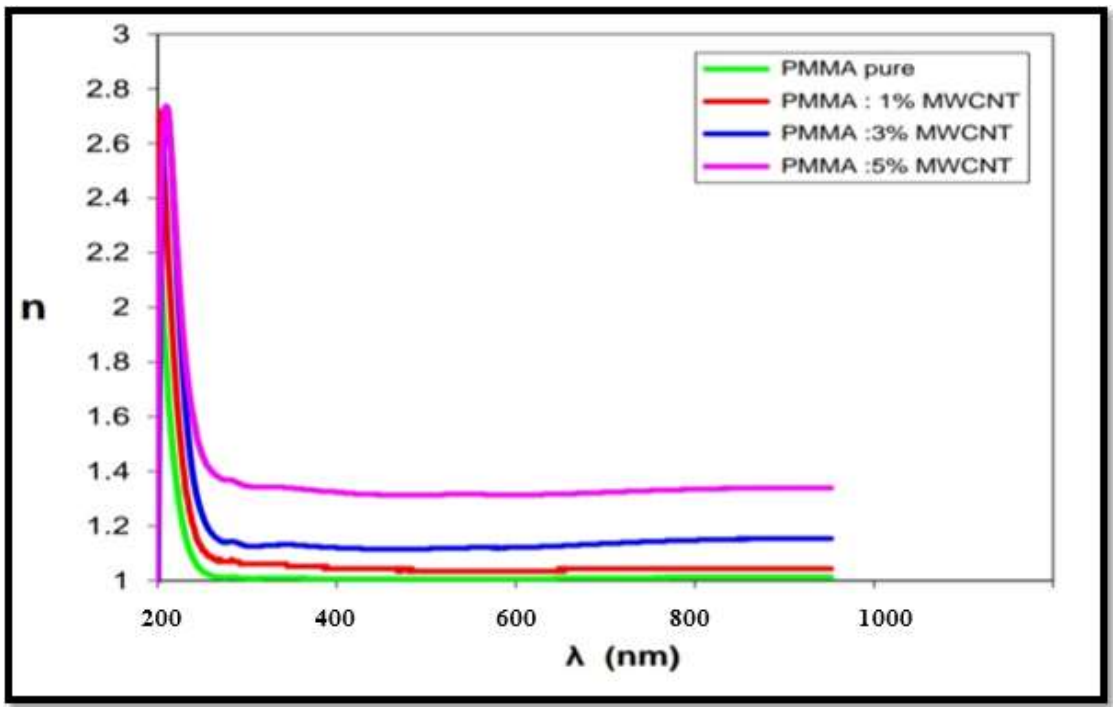

Fig. (4.12) The refractive index variation with the wave-length for the doped as well as pure PMMA films.

4.3.7 Extinction Coefficient:

The measured values of extinction coefficient (k) of (PMMA) preceding and following the process of doping could be clarified as in Fig. (4.13).

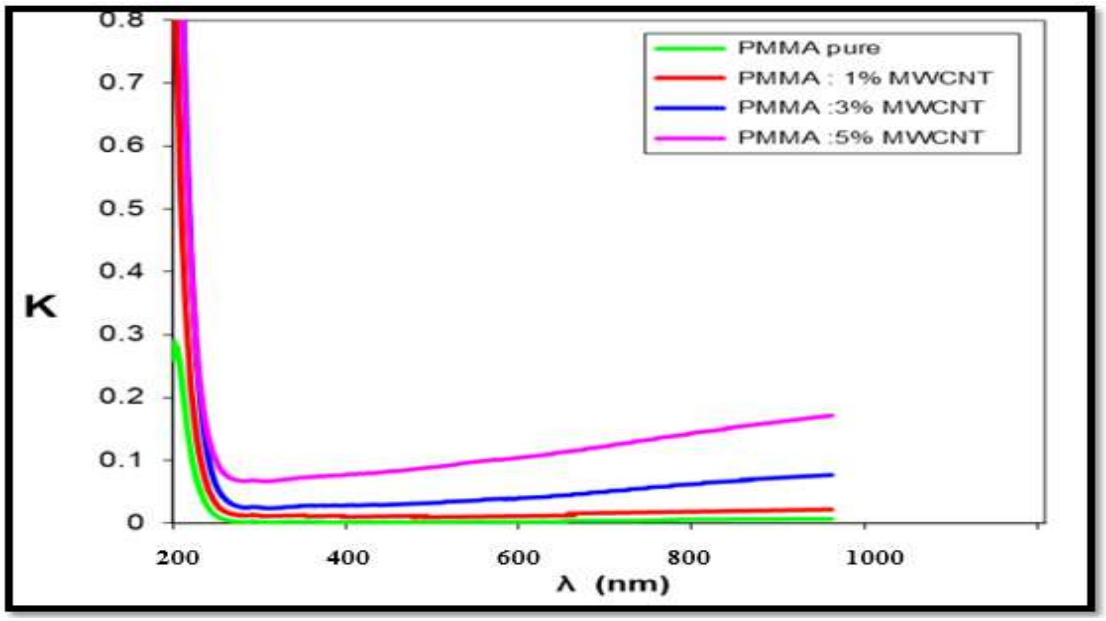

Fig. (4.13) The variation of the extinction coefficient for the pure as well as the doped films of the PMMA.

4.3.8 Real and Imaginary Parts of Dielectric Constant:

Such behavior is corresponding to absorbing centers' density like the excitation transition, impurity absorption, and other defects in crystal lattice dependent upon sample preparation conditions. Dielectric constant has been characterized as imaginary (ε_2) part and real (ε_1) part of dielectric constant have been associated with values of n and k. The values of $\varepsilon 2$ and $\varepsilon 1$ have been computed with the use of the formulas below [26].

$$\varepsilon_1 = n^2 - k^2 \qquad (4.2)$$

$$\varepsilon_2 = 2nk \qquad (4.3)$$

$$(\omega) = \varepsilon_1(\omega) + i\varepsilon_2(\omega) \qquad (4.4)$$

The real and imaginary of dielectric constant of (PMAA) before and after doping are calculated using the equations (4.3, 4.4) and shown in Figures (4.14 and 4.15) for the pure and the doped films. Values of $\varepsilon 1$ are higher in comparison with the $\varepsilon 2$ values. It has been observed that values of $\varepsilon 1$ & $\varepsilon 2$ have been increased with the increase in the wave-length and with MWCNT doping concentrations.

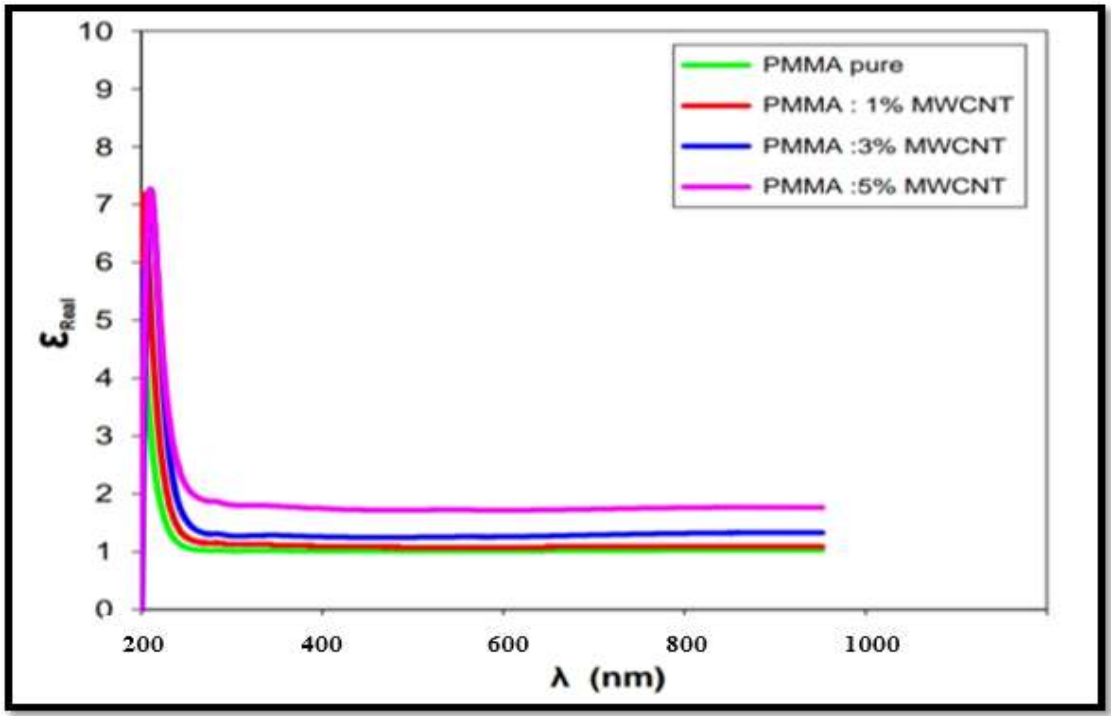

Fig. (4.14) The variations of the dielectric constant's real part with wave-length for the pure as well as the doped films of the PMMA.

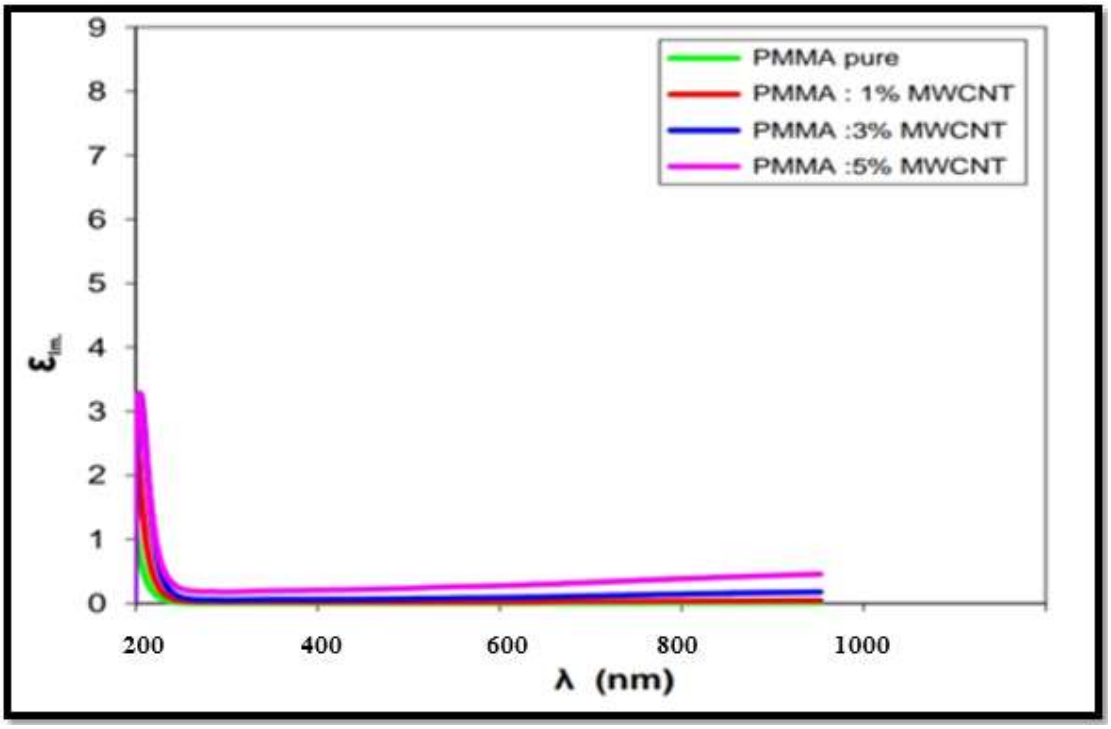

Fig. (4.15) The variations of the dielectric constant's imaginary part with the wave-length for the pure as well as the doped films of the PMMA.

4.3.9 Optical connectivity (σ) for pure and doped thin films:

Optical connectivity (σ) this value has been computed based on the equation below [28]:

$$\sigma = \varepsilon_2 \omega \varepsilon_0 \qquad (4.5)$$

Where: σ represents the optical conduction and ε_2 represents imaginary dielectric constant with ω represents permittivity of the space. Figure (4.16) illustrates changes of the optical conductivity as a wave-length function where maximal conductivity in UV range of electro-magnetic spectrum, and it is decreased with the increase in the value of the wave-length, Based on the graph, it is expected that when the MWCNTs content increases. The optical connectivity of the nano-composites would be vary continuously from the pure PMMA to pure MWCNTs when the two materials were combined . The MWCNTs and PMMA were mixed effectively and connected in series showing a dramatic increase in the Optical Connectivity when the MWCNTs exceeds 2.0 wt.%.

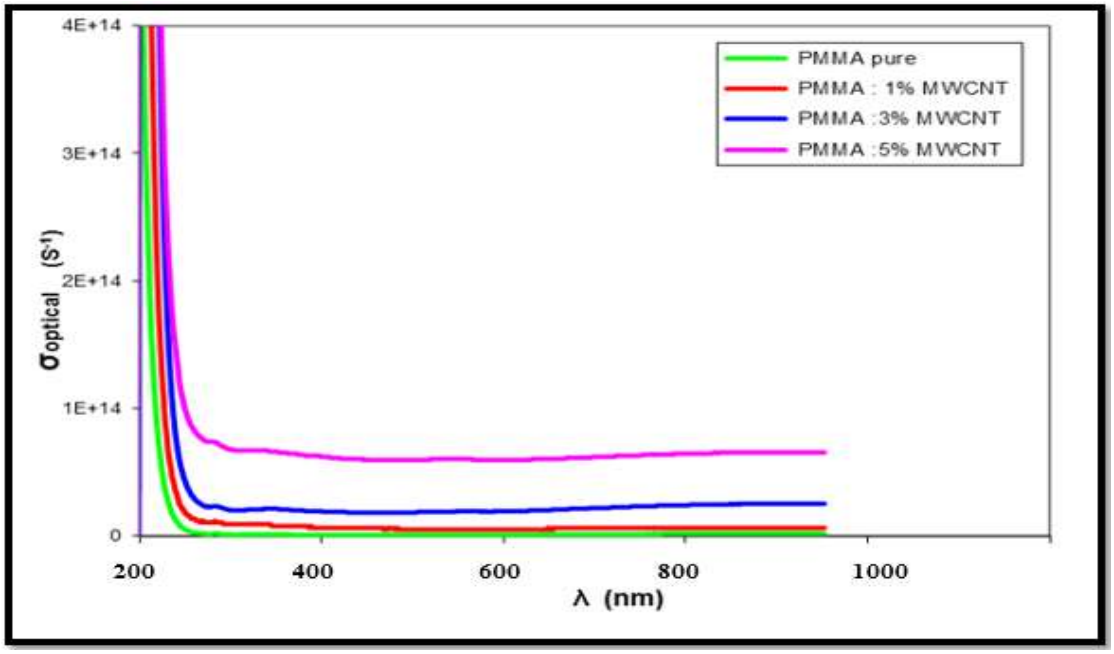

Fig. (4.16) The PMMA/MWCNTS nanocomposites optical connectivity

4.4 Sensing Properties for pure and doped thin films:

4.4.1 Gas Sensitivity for NO_2:

For the samples prepared for the applications of the sensor, the sensitivity of doped PMMA/MWCNTs thin films could be measured through calculating the changes in the resistance of the given thin film in both air and gas. Fig. (4.17) and (4.18) show the gas sensitivity of doped PMMA/MWCNTs thin films deposition on glass substrate with gas concentration (100ppm for No_2 gas) doped PMMA/MWCNTs thin film show increasing in sensitivity reaches to (8.15%) which belong to doping concentration (1,3,5 wt.% MWCNTs) respectively, which is in agreements with findings of other works .

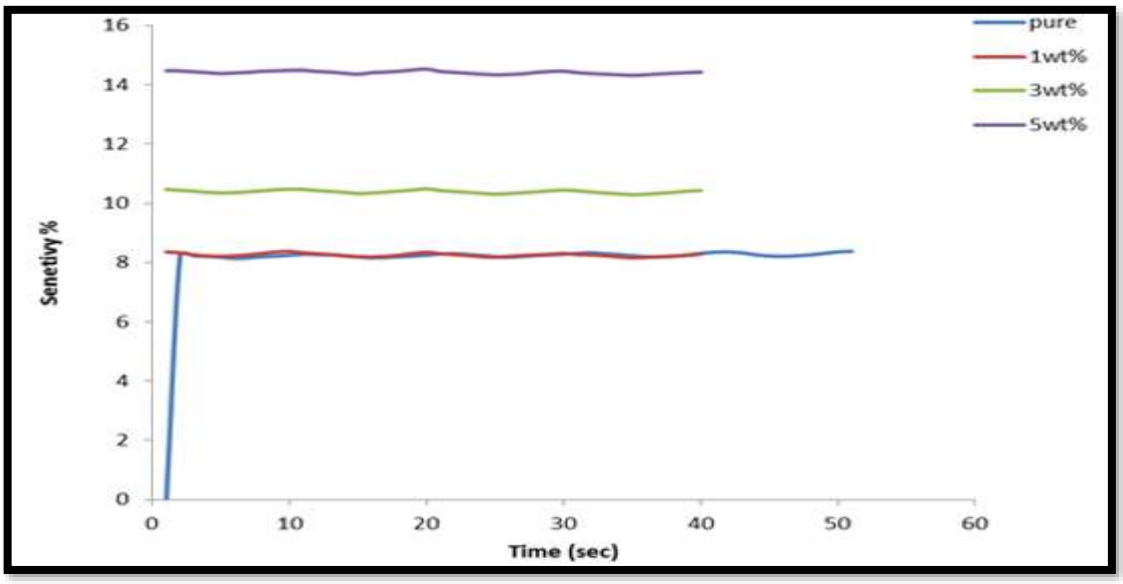

Fig. (4.17) The sensitivity of doped PMMA films for NO_2 gas.

4.4.2 Gas Sensitivity for NH_3:

The Figure (4. 18) shows the gas sensitivity of doped PMMA on glass substrate at different concentration (1, 3, 5) wt % became higher while increasing the doping concatenation since the more doping concentration the bigger grain size and the roughness of surface decreases leading to decreases in the sensitivity of film .

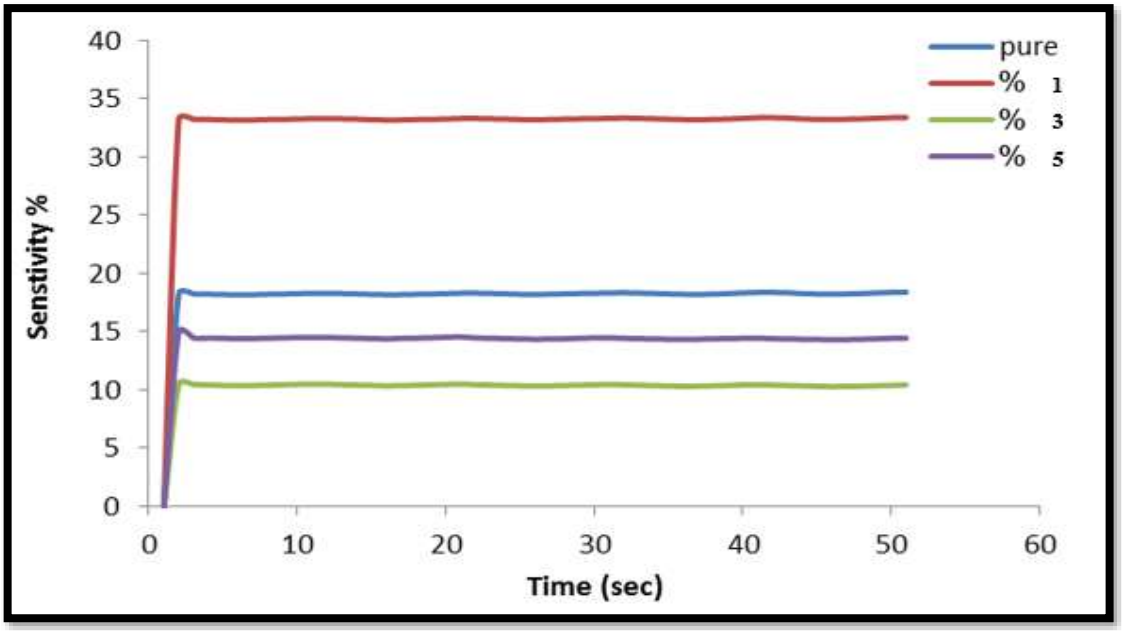

Fig. (4.18) The sensitivity of doped PMMA films for NH_3 gas.

4.5 Conclusion:

1- The XRD and FTIR analysis have proven that the prepared material of PMMA with MWCNTs as additive was thin films and no new chemical compounds found.

2- As the MWCNTS increased the absorption of wavelength increase especially in UV region, this means that the PMMA/MWCNTs thin films will improve the weather ability of polymer so it can be used as a protection layer in the solar cells application.

3- As the MWCNTs particles increase in PMMA matrix then the energy gap suffered decreased in its value and the composite become less insulating and approach towards the semiconductor.

4- Increasing MWCNTs particles in the PMMA matrix increases the values of dielectric constant.

5- The Atomic Force Microscopic (AFM) images have shown that all of the films are uniformed and there is no any significant difference between all of the concentrations.

6- The sensitivity for two types of gases (NO_2, NH_3) for PMMA/MWCNTs thin films are well increased because of increasing doping concentration.

4.6 Future Work

Due to the experimental results in the present work and for a complementary identification of PMMA and its thin films we can suggest these future work:

1- Studying the thermal and mechanical behavior of PMMA and its composites.
2- Studying the electrical properties of PMMA and its composites under applying alternative voltage.
3- Studying the electrical and optical properties of PMMA with other metal oxides.
4- Investigating the electrical properties of polymer enhanced with Nano silver approach to make conductive polymer.

References

References

[1] Sybrand van der Zwaag, "Self Healing Materials", Springer, Netherland, 2007.

[2] Evgeny V. Morozov, Valery Vasiliev, "Advanced Mechanics of Composite Materials and Structural", Elsevier, 2013.

[3] William D. Callister, Jr. , David G. Rethwisch, "Fundamentals of Materials Science and Engineering", John Willy and sons, 2008.

[4] David I. Bower, "An Introduction to Polymer Physics", Cambridge University press, 2002.

[5] Prof. Premamoy Ghosh, "Fundamentals of Polymer Science", Polymer Study center, 2006.

[6] Robert O. Ebewele, "Polymers Science and Technology", CRC Press, 2000.

[7] Joel R. Fried, "Polymer Science and Technology", Prentice Hall, 2014.

[8] Fred W. Billmeyer, "Text Book of Polymer Science", John Willy & sons ,1984.

[9] Shaw Ling Hsu, "Polymer Data Handbook", Oxford university press, 1999.

[10] D.W. Van Krevelen, "Properties of Polymers", Elsever, 2009

[11] Stevens, Malcolm P., "Polymer Chemistry: An Introduction", Oxford university press, 1998.

[12] John Brydson, "Plastic Materials", Butterworth-Heinemann press, 7th Edition, 1999.

[13] Kumar DA, Abdul Kalam SD, Design, "Analysis and Comparison between the Conventional Materials with Composite Material of the Leaf Springs", Fluid Mech Open Acc, Vol 3, No. 3:127pp.2476-2296, 2016.

[14] P. K. Mallick, "Composite Engineering Handbook", Marcel Dekker, 1997.

[15] C. Klingshirn, ZnO Material, "Physics and Application" ChemPhys Chem, Vol. 8,pp. 782 – 803, 2007.

[16] Claus F. Klingshirn, Andreas Waag, Axel Hoffmann, Jean Geurts, "Zinc Oxide: From Fundamental Properties Towards Novel Applications", Springer, 2010.

[17] Zhong Lin Wang, "Zinc oxide Nanostructures: Growth, Properties and Applications", J. Phys.: Condens. Matter, 16, R829–R858, 2004.

[18] Xiaoge Gregory Zhang, "Corrosion and Electrochemistry of Zinc", Plenum Press, 1996

[19] Hong-Wen Wang, Chain-Fang Shieh, Kung-Chin Chang, Hsuan Chih Chu, "Synthesis and Dielectric Properties of Poly(methyl methacrylate) Clay Nanocomposite", Vol. 97, 2175–2181, 2005.

[20] E. Tang, Guoxiang Cheng, Xiaolu Ma, "Preparation of Nano ZnO /PMMA Composite Particles via Grafting of the Copolymer onto the Surface of Zinc Oxide Nanoparticles" , Powder Technology, 161, 209–214, 2006.

[21] Mustafa M. Demir, Mine Memesa, Patrice Castignolles, Gerhard Wegner, "PMMA/Zinc Oxide Nanocomposites Prepared by In-Situ Bulk Polymerization", Macromol. Rapid Commun., 27, 763–770, 2006.

[22] R.Y. Hong, J.Z. Qian, J.X. Cao, "Synthesis and Characterization of PMMA Grafted ZnO Nanoparticles", Powder Technology ,163, 160–168, 2006.

[23] Ahmad A.H., Awatif A.M. and Zeid Abdul-Majied N., "Dopping Effect On Optical Constants of Poly methyl methacrylate (PMMA)" , Eng. & Technology, Vol.25, No.4, 2007.

[24] Zainab A., "Effect of Nickel Salt on Electrical Properties of Poly Methyl Methacrylate", Journal of College of Education, Vol. 3, pp.321-327, 2008.

[25] Moriyuki Sato, Akihito Kawata, Shigekazu Morito, Yuzuru Sato, Isao Yamaguchi, "Preparation and Properties of Polymer/Zinc Oxide Nanocomposites using Functionalized Zinc Oxide Quantum Dots", European Polymer Journal Vol.44, pp.3430–3438, 2008.

[26] Bahaa Hussain, Marwa Abdul-Muhsien, Ahmad Hashim, "Study of Some Electrical Properties for PMMA-TiO2 Composites", attidella Fondazione Giorgio Ronchi Anno LXVI No.1, 2010.

[27] Muhammad Hameed Abdul-Allah, Sami Salman Chiad, Nadir Fadhil Habubi, "The Effect of Iron Chromate on the Optical Properties of PMMA Films", Diyala journal for pure science, Vol.6, No.2, 2010.

[28] R. Sreeja, Jobina John, P.M. Aneesh, M.K. Jayaraj, "Linear and Nonlinear Optical Properties of Luminescent ZnO Nanoparticles Embedded in PMMA Matrix", Optics Communications, Vol.283, pp. 2908– 2913, 2010.

[29] B. Kulyka, V. Kapustianyka, V. Tsybulskyya, O. Krupkab, B. Sahraouic, "Optical Properties of ZnO/PMMA Nanocomposite Films", Journal of Alloys and Compounds, Vol.502, pp.24–27, 2010.

[30] Gaurang Patel, M.B.Sureshkumar, Purvi Patel, "Effect of TiO2 on Optical Properties of PMMA: An Optical Characterization, Advanced Materials Research", Vols. 383-390, pp. 3249-3256, 2012.

[31] P.P. Jeeju a, S. Jayalekshmi, K. Chandrasekharan, P. Sudheesh , "Enhanced Linear and Nonlinear Optical Properties of Thermally Stable ZnO/PolyStyrene/PolyMethyl Methacrylate Nanocomposite" , Thin Solid Films, Vol. 531, PP. 378–384, 2013.

[32] Yewei Zhang, Shendong Zhuang, Xiaoyong Xu, Jingguo Hu, "Transparent and UV-Shielding ZnO/PMMA Nanocomposite Films", Optical Materials, Vol.36, pp. 169–172, 2013.

[33] Khalid Al-Ammar, Ahmed Hashim, Maithem Husaien, “Synthesis and Study of Optical Properties of (PMMA-CrCl2) Composites”, Chemical and Materials Engineering, 1(3), 85-87, 2013.

[34] Basavaraja Sannakki and Anita, “Dielectric Properties of PMMA and its composites with ZrO2”, Physics Procedia, Vol.49, pp. 15 – 26, 2013.

[35] Farooq Momtaz Abd Omran, “Study of the Electrical Properties of (PMMA-Ag) and (PMMA-Ti) nanocomposites”, M.Sc Thesis, Babylon University, College of Education for Pure Sciences, 2014.

[36] Somayeh Fardindoost ,AzamIrajizad, Fereshteh Rahimi and Roghayeh Roghayeh Ghasempou ,"Pd doped WO3 films prepared by sol–gel process for hydrogen sensing". international-journal-of-hydrogen-energy , vol .35, No, 2 pp. 854-860 ,2010.

[37] Payam Molla-Abbasi, Seyed Reza Ghaffarian and Ehsan Danesh ,"Porous carbon nanotube/PMMA conductive composites as a sensitive layer in vapor sensors". Smart Materials and Structures, Vol,20, No,10 ,2011.

[38] Bin Sun, Yun-Ze Long Zhao-Jun Chen, Shu-Liang Liu, Hong-Di Zhang, Jun-Cheng Zhang and Wen-Peng Han."Recent advances in flexible and stretchable electronic devices via electrospinning". J. Mater. Chem. C, Vol.2, pp.1209-1219, 2014.

[39] Souvik Basaka , Sandip Mondala , Suddhasattya Deya , Plaban Bhattacharyab , Achintya Sahab , Vinay Deep Punethac , Ali Abbasd and Nanda Gopal Sahoo ." Fabrication of b-cyclodextrin-mediated single bimolecular inclusion complex: characterization, molecular docking, in-vitro release and bioavailability studies for gefitinib and simvastatin conjugate " 2017.

[40] Bharti, Madhu Lata, Sanjay Dutt, Rakesh Raturi, and Veena Joshi. “Structural Modifications of PMMA and PMMA/CNT Matrix by Swift Heavy Ions Irradiation.” In IOP Conference Series: Materials Science and Engineering, IOP Publishing, 12093. 2017

[41] Subhendu Bhandari and Prashant Gupta ,"Chemical Depolymerization of Polyurethane Foam via Ammon lysis and amino lysis". Recycling of Polyurethane Foams ,Plastics Design Library, Pages 77-87, 2018.

[42] Shujahadeen B. Aziza ,b, M.H. Hamsanc, M.A. Brzad, M.F.Z. Kadirc, Rebar T. Abdulwahide, Hewa O. Ghareebf and H.J. Woog," Fabrication of energy storage EDLC device based on CS:PEO polymer blend electrolytes with high Li+ ion transference number, Results in Physics ,Vol. 15 No.102584 ,pp. 24-34 ,2019.

[43] Mergen, Ömer Bahadır, Ertan Arda, and Gülşen Akın Evingür. “Electrical, Mechanical, and Optical Changes in MWCNT-Doped PMMA Composite Films.” Journal of Composite Materials 54(18): 2449–59, 2020.

[44] R. A. Qazi Qazi, Raina Aman Khattak, Rozina Ali Shah, Luqman Ullah, Rizwan Khan, Muhammad Sufaid Sadiq, Muhammad Hessien, Mahmoud M El-Bahy, Zeinhom M., “Effect of MWCNTs Functionalization on Thermal, Electrical, and Ammonia-Sensing Properties of MWCNTs/PMMA and PHB/MWCNTs/PMMA Thin Films Nanocomposites,” Nanomaterials, vol. 11, no. 10, p. 2625, 2021.

[45] Nassier, Lamis Faaz, and Mohammed Hadi Shinen. “Study of the Optical Properties of Poly (Methyl Methacrylate)(PMMA) by Using Spin Coating Method.” Materials Today: Proceedings 60: 1660–64.2022.

[46] Iijima S. Helical microtubules of graphitic carbon. Nature Vol, 354:pp.56–8.1991.

[47] Shah KA, Tali BA. "Synthesis of carbon nanotubes by catalytic chemical vapour deposition: a review on carbon sources, catalysts and substrates". Mater Sci Semicond Process Vol;41:pp.67–82.2014.

[48] Anjidani M, Moghaddam HM, Ojani R. "Binder-free MWCNT/TiO2 multilayer nanocomposite as an efficient thin interfacial layer for photo anode of dye sensitized solar cell". Mater Sci Semicond Process Vol;71:pp.20–8.2017.

[49] Sireesha M, Babu VJ, Ramakrishna S. Functionalized carbon nanotubes in bio- world: applications, limitations and future directions. Mater Sci Eng, B Vol.;223:pp.43–63.2017.

[50] Seidel R, Graham AP, Unger E, Duesberg GS, Liebau M, Steinhoegl W, et al. "High- current nanotube transistors". Nano Lett Vol;4:pp.831–4.2004.

[51] Wang C, Waje M, Wang X, Tang JM, Haddon RC, Yan Y." Proton exchange membrane fuel cells with carbon nanotube based electrodes". Nano Lett Vol.;4:pp.345–8.2004.

[52] Zhang T, Mubeen S, Myung NV, Deshusses MA. Recent progress in carbon nanotube- based gas sensors. Nanotechnology". Vol.;19:pp.332001.2008.

[53] Rossi CB, Micheli GD, Carrara S. Electrochemical detection of anti-breast-cancer agents in human serum by cytochrome P450-coated carbon nanotubes. Sensors Vol,;12:pp.6520–37.2012.

[54] Zhu S, Song Y, Zhao X, Shao J, Zhang J, Yang B. "The photoluminescence mechanism in carbon dots (graphene quantum dots, carbon nanodots, and polymer dots)". Current state and future perspective. Nano Res ,Vol.8:pp.355–81.2015.

[55] Essner JB, Baker GA. The emerging roles of carbon dots in solar photovoltaics: a critical review. Environ Sci Nano Vol,4:pp.1216–63.2017.

[56] Malfatti L, Innocenzi P. Sol-Gel chemistry for carbon dots". Chem Rec Vol,pp.18:1192–202.2018.

[57] Ding Y, Zhang F, Xu J, Miao Y, Yang Y, Liu X, et al. "Synthesis of short-chain passivated carbon quantum dots as the light emitting layer towards electro- luminescence". RSC Adv .Vol,7:pp.28754.2017.

[58] R. Deokate, S. Salunkhe, G. Agawane, B. Pawar, S. Pawar, K. Rajpure , A. Moholkar, and J. Kim, "Structural, optical and electrical properties of chemically sprayed nanosized gallium doped CdO thin films," Journal of Alloys and Compounds, vol. 496, no. 1-2, pp. 357-363, 2010.

[59] R. John Bosco Balaguru" Mimic of a Gas Sensor, Metal Oxide Gas Sensing Mechanism Factors Influencing the Sensor Performance and Role of nanomaterials based gas sensors" NPTEL – Electrical and Electronics Engineering – Semiconductor Nanodevices (2004) 1-30.

[60] M. Birkholz, Thin Film Analysis by X-Ray Scattering, WILET-VCH Verlag GmbH & Co, Weinheim, (2006).

[61] Bfnan F. , Xhengguo Jin , Yong N. , Haiyan D. and Tao Wang , "Microstructure, Optical and Optoelectrical Properties of Mesoporous SnO2 Films by Hydrolysis-limited Sol–Gel Process With Different Inhibitors", Thin Solid Films ,Vol. 410, pp. 3634–3637, (1999).

الخلاصة:

في هذه الدراسة تم تحضير اغشية PMMA مع الانابيب الكاربونية النانوية المتعددة الجدران وبنسب (1% و 3% و 5%)، تم دراسة طيف (FTIR) للأغشية المحضرة لتحديد المجموعات النشطة للروابط الكيميائية ، أظهرت نتائج التحليل أن البوليمرهو بولي ميثيل (ميثاكريلات) , كما ان التطعيم لم يؤثر على خصائص بولي ميثيل (ميثاكريلات).

تم دراسة حيود الأشعة السينية (XRD) واظهرت النتائج أن الأفلام المحضرة غير متبلورة، وأظهرت النتائج أن انابيب الكاربون لم تؤثر على الخواص التركيبية للبوليمر بولي ميثيل (ميثاكريلات) .

تم فحص شكل السطح للأغشية الرقيقة باستخدام تقنية مجهر القوة الذرية (AFM). أظهرت النتائج أن المادة كانت متجانسة. تناقص معدل الخشونة، وقيمة متوسط الجذر (RMS) وزيادة متوسط حجم الحبيبات مع زيادة تركيز انابيب الكاربون النانوية.

تم فحص الخواص البصرية للأغشية المحضرة من خلال الحصول على طيف النفاذية في مناطق الأشعة فوق البنفسجية كدالة لطول الموجة من (200 - 1000) نانومتر. تتضمن الخواص البصرية قياس طيف الامتصاصية وطيف النفاذية كدالة للطول الموجي لمزيج PMMA مع الأنابيب النانوية الكربونية متعددة الجدران ثم حساب معامل الامتصاص والثوابت البصرية الأخرى. وتتزايد قيم الامتصاص، ومعامل الامتصاص، وقيم معامل الانكسار للبوليمر النقي والمشوب مع زيادة نسبة تركيزات انابيب الكاربون النانوية. تظهر النتائج انخفاض قيم النفاذية مع كل نسبة من انابيب الكاربون، وقيمة الانعكاسية تزداد مع زيادة نسبة التركيز، كما أظهرت النتائج انخفاض فجوة الطاقة للانتقال المباشر المسموح مع زيادة نسبة تركيز انابيب الكاربون النانوية، تم الحصول على قيم فجوة الطاقة وكانت تساوي من (3.88 ev الى 3.52 ev) للبوليمر النقي بمعدلات مختلفة من الأنابيب الكربونية.

بالنسبة للأغشية الرقيقة النقية والمشوبة، لوحظ أنه مع زيادة تركيز المادة المشوبة تزداد الحساسية لنوعين من الغازات (NH_3 / NO_2) لأنه مع زيادة تركيز المادة المشوبة يزداد الحجم الحبيبي وتقل خشونة السطح مما يؤدي إلى زيادة حساسية الاغشية الرقيقة.

جمهورية العراق
وزارة التعليم العالي والبحث العلمي
جامعة بابل / كلية العلوم
قسم الفيزياء

تحضير وتشخيص أغشية رقيقه (PMMA – MWCNT) وتطبيقاتها في متحسسات الغاز

رسالة مقدمة الى
مجلس كلية العلوم – جامعة بابل
وهي جزء من متطلبات نيل درجة الماجستيرفي العلوم /الفيزياء

من قبل

محمد هاتف صالح مهدي

بكالوريوس علوم في الفيزياء /2007

إشراف

أ.د محمد هادي شنين **أ.م.د. معن عبد الامير صالح**

١٤٤٤هـ ٢٠٢٢م